

Prompt neutron decay measurements
using a microcomputer-based
data acquisition system

by

Douglas John Meyer

A Thesis Submitted to the
Graduate Faculty in Partial Fulfillment of
The Requirements for the Degree of

MASTER OF SCIENCE

Department: Chemical Engineering and Nuclear Engineering
Major: Nuclear Engineering

Signatures have been redacted for privacy

Iowa State University
Ames, Iowa

1978

TABLE OF CONTENTS

	Page
NOMENCLATURE	vi
I. INTRODUCTION	1
II. LITERATURE REVIEW	5
III. THEORY	9
A. Derivation of the Autocorrelation Function	9
B. Data Collection Methods	14
IV. EXPERIMENT	20
A. Data Acquisition System	20
B. Selection of Detector and Optimum Operating Parameters	29
C. Analysis of Results	45
V. CONCLUSIONS	54
VI. REFERENCES	57
VII. ACKNOWLEDGMENTS	59
VIII. APPENDIX A: COUNTER-TIMER PERIPHERAL	60
IX. APPENDIX B: PROMPT NEUTRON DECAY PLOTS	66
X. APPENDIX C: DATA COLLECTION ROUTINE ROSSI.SRC	72
A. Description of ROSSI.SRC	72
B. Source Code Listing of ROSSI.SRC	76
XI. APPENDIX D: DATA COLLECTION ROUTINE VARMEN.SRC	87
A. Description of VARMEN.SRC	87
B. Source Code Listing of VARMEN.SRC	91

LIST OF FIGURES

	Page
3.1. Consolidated acquisition-analysis program based on the Rossi Alpha Method	15
3.2. Consolidated acquisition-analysis program based on a variance to mean approach	18
4.1. KIM-1 microcomputer	21
4.2. Data acquisition system	24
4.3. Flowsheet for data collection routine ROSSI.SRC	25
4.4. Channel width for various hexadecimal constants stored in timer routine	31
4.5. Microcomputer channel width deviation	33
4.6. Geometrical arrangement of the UTR-10 coupled core reactor	37
4.7. Response of ^3He and BF_3 detectors to thermal neutrons and gammas	39
4.8. Figure of merit for various detector arrangements	40
4.9. Influence of the average count rate on data collection times	43
4.10. Effect of high voltage on count rate for ^3He and BF_3 detectors	44
4.11. Decay of prompt neutrons with all control rods inserted	46
4.12. Prompt neutron decay constant for various reactor configurations	48
8.1. Counter-timer peripheral	62
9.1. Prompt neutron decay with safety 1 50 percent withdrawn and safety 2 fully inserted	67

	Page
9.2. Prompt neutron decay with safety 1 fully withdrawn and safety 2 fully inserted	68
9.3. Prompt neutron decay with safety 1 fully withdrawn and safety 2 30 percent withdrawn	69
9.4. Prompt neutron decay with safety 1 fully withdrawn and safety 2 60 percent withdrawn	70
9.5. Prompt neutron decay with safety 1 fully withdrawn and safety 2 fully withdrawn	71
11.1. Flowsheet for VARMEN.SRC	88

LIST OF TABLES

	Page
4.1. Experimental results, degree of reactor subcriticality	50
4.2. Control rod reactivity worths	51
8.1. PIA 6530-003 data bit definitions	64
8.2. Useful hexadecimal values for control of counter-timer peripheral	65

NOMENCLATURE

Acronyms

BCD	Binary coded decimal
FFT	Fast Fourier transform
IRQ	Interrupt request
MCA	Multichannel analyzer
NMI	Nonmaskable interrupt
PIA	Peripheral interface adaptor
PSD	Power spectral density
RAM	Random access memory
ROM	Read-only memory

RomanUnits

c	Mean count rate	counts/s
C	Delayed neutron precursor density	nuclei/cm ³
C _s	Steady state delayed neutron precursor density	nuclei/cm ³
k	Neutron multiplication constant	
l	Prompt neutron lifetime	s
n	Neutron density	neutrons/cm ³
n _B	Uncorrelated neutron density	neutrons/cm ³
n _O	Prompt neutron density following a fission	neutrons/cm ³
n _S	Steady state neutron density	neutrons/cm ³
n _T	Total neutron density	neutrons/cm ³

N	Number of triggered scans	
N_{ch}	Number of channels	
N_T	Time integrated neutron density	neutrons s/cm ³
S	Source rate	neutrons/s
t_{ch}	Channel width	s
t_{coll}	Data collection time	minutes
t_{cyc}	Time required for program to cycle back to initial starting position	s
t_T	Total time required per scan	s
t_w	Average waiting time for a trigger neutron detection	s
t	Time	s

<u>Greek</u>		<u>Units</u>
α	Prompt neutron decay constant	radians/s
α_0	Prompt neutron decay constant at delayed critical (Rossi Alpha)	radians/s
β	Delayed neutron fraction	
ϵ	Detector efficiency	counts/ fission
η	Detector figure of merit	
λ	One group delayed neutron precursor decay constant	s ⁻¹
Λ	Neutron generation time (l/k)	s
ν	Average number of neutrons per fission	
ρ	Reactivity ($\frac{k-1}{k}$)	

$\rho(\$)$

Reactivity

dollars

τ

Gate time

s

I. INTRODUCTION

The recent trend in data acquisition equipment has been toward the consolidation of information gathering and reduction into a single unit. Developments in large scale integrated circuit technology which have resulted in the widespread availability of microprocessors, read-only memories, and peripheral interfacing devices are largely responsible for this trend. Characteristics of this type of equipment generally include analog signal inputs, an analog to digital converter, random access memory in which to store the digitized data, a read-only memory which contains machine language programs for supervising the data collection and performing the analysis, a microprocessor, and provisions to output the result to the operator. One of the most notable devices in this category is the Power Spectral Density Analyzer (sometimes referred to as a FFT analyzer) which accepts an analog noise signal, digitizes this signal at a selected frequency, and performs fast Fourier transforms on the digitized data. After collecting many data ensembles from the noise signal the resulting power spectral density is visually displayed on a cathode ray tube. Some of these FFT analyzers have provisions for two noise inputs, therefore making possible the determination of cross power spectral densities as well as the individual PSD for each signal.

The development of self-contained data acquisition-data reduction equipment requiring a minimum of external data manipulation permits analyses to be performed by technicians who may not be completely familiar with the theoretical aspects of the analysis. Increased flexibility in testing schedules due to the relaxed qualification requirements of the operator is one advantage resulting from the implementation of this type of equipment.

The expense of a consolidated data acquisition-data reduction system (approximately \$30,000 for a FFT analyzer) may be easily justified in a large industrial complex but at a university, where primary emphasis is placed upon instructional laboratory course work and research, such an investment in a single piece of equipment solely dedicated to one type of analysis is unacceptable. Fortunately the advent of the microprocessor has also made available extremely low cost computer systems which may be used for a variety of applications by interfacing comparatively inexpensive peripheral devices to the computer bus and developing the necessary software to support these devices. Thus a highly versatile piece of laboratory equipment could be obtained at the price of a single dedicated instrument.

Recently an experiment to measure prompt neutron decay constants in the Iowa State University UTR-10 Research Reactor has received some attention. The prompt neutron population in

a point reactor following a fission event has been found to decay exponentially with time if delayed neutrons are neglected [17]. Therefore, if the neutron population following the detection of a neutron pulse is measured for discrete periods of time with a multichannel analyzer, an exponential decay is expected. This procedure, known as the Rossi Alpha Method [19], is one means of obtaining prompt neutron decay constants and the value of β/λ (the Rossi Alpha) for a point reactor model. Usually a large number of scans triggered by a neutron detection are summed to obtain a statistically significant result.

One of the primary reasons many experimenters were unsuccessful in using a multichannel analyzer for prompt neutron decay measurements was due to the large dead times between adjacent channels. The implementation of a microcomputer in conjunction with an external timer and two counters has a large potential for overcoming this problem. If a sufficiently expanded microcomputer were used, data reduction could be performed during the course of the experiment which would provide an immediate indication of how well the experiment was progressing.

This study will be primarily devoted to the identification of the advantages and limitations inherent in the measurement of prompt neutron decay constants using a microprocessor-based

instrument. The applicability of using a point reactor model for the Iowa State University UTR-10 Reactor will also be considered.

II. LITERATURE REVIEW

The measurement of prompt neutron decay constants resulting from observing the time distribution of neutron detections following a randomly-chosen trigger detection was first suggested by Bruno Rossi [19]. Orndoff [17] derived an expression for the probability of subsequent detections in time intervals following an initial detection at $t = 0$. Orndoff's experiments on GODIVA-1 employed a series of ten delay lines and coincidence circuits in order to analyze the time distribution of a sequence of pulses with respect to each of the individual pulses in the sequence. Since this experiment was performed on a fast assembly, delays of $1\mu\text{s}$ were used between the coincidence circuits.

Brunson et al. [5] measured the time between pairs of neutron detections to obtain prompt neutron decay constants for various fast critical assemblies in ZPR-III. Since the time analyzer was reset each time the second pulse in a pair was detected, the later channels in the analyzer were examined less often than the earlier channels. Brunson suggested an appropriate correction factor to account for this anomaly.

Bryce [7] used the Rossi Alpha Method to measure prompt neutron decays in a thermal reactor at Cornell University. A BF_3 detector was located at the core periphery and using channel widths of $160\mu\text{s}$ the value of the Rossi Alpha for this core was found to be $161 \pm 5 \text{ rad./s}$. Measurements of

control rod worth based on prompt neutron decay constants were very similar to results obtained from positive period measurements using the inhour equation.

Brunson et al. [6] used the Rossi Alpha Method for measurements on a beryllium reflected ZPR-III assembly. They employed two analyzers, one having a $2\mu\text{s}$ channel width and the other a $10\mu\text{s}$ channel width. This allowed the measurement of a second decay constant which resulted from the presence of the reflector. The smaller decay constant was attributed to neutrons having spent time in the reflector (ℓ is effectively increased, therefore β/ℓ decreases) while the longer decay constant was representative of an unreflected core. Two BF_3 detectors located within the core were used to obtain these measurements.

An entirely different approach based on the statistical nature of neutron counts over various lengths of time was presented by Thie [22]. This method entails obtaining ratios of the variance to the mean number of counts present in each channel for a given channel width or gate time. Data sets are collected for various gate times after which the variance to mean ratios, as a function of gate time, are fit to an expression in which the prompt neutron decay constant is one of the parameters. Albrecht [1] performed an experiment with a thermal reactor based on a variance to mean analysis. Using gate times from 1ms to 10s and including two groups of

delayed neutrons in the fitting function, he was able to show that if gate times are restricted to less than 100ms delayed neutron effects may be ignored.

The application of computers dedicated to data acquisition and analysis has only recently come to pass due to recent cost reductions in these systems. De Clercq et al. [10] constructed a pulse height analysis system based on a PDP 11 10-E minicomputer using a CAMAC interface. This is one of the most elegant systems of its type and is quite expensive.

A micro-CAMAC system based on an INTEL 8080A micro-processor for use in gamma spectrometry has been developed by Kumahara et al. [12]. The micro-CAMAC system is used to transfer data from several multichannel analyzers to the microcomputer for analysis. The use of a microcomputer and micro-CAMAC peripheral greatly reduces the price of the system in comparison to De Clercq's pulse height analyzer.

Silberberg [20] developed a portable neutron spectrometer based on a M6800 microprocessor. By implementing a machine language floating point package system memory requirements were small and calculations were performed quickly. A pulse height distribution analysis could be processed in approximately one second.

A microprocessor controlled reactivity meter was developed by Auerbach and Carpenter [2]. A General Instrument 1600 microprocessor was used to achieve real time reactivity monitoring.

Reactivities were obtained by solving the inverse kinetics equations using the digitized output of a neutron detector. Reactivity values were updated every 0.1 second. Since the only required process signal was a digital output of the reactor power history, this device is readily adaptable to other reactor installations.

III. THEORY

A. Derivation of the Autocorrelation Function

Spatially independent reactor kinetic responses are most conveniently represented by the point kinetics equations. If the times of interest are very short with respect to the shortest-lived delayed neutron precursors, delayed neutron effects may be neglected. The behavior of the prompt neutron density with time is [11]

$$\frac{dn}{dt} = \frac{\rho - \beta}{\Lambda} n \quad (3.1)$$

where the symbols used have their usual meanings. Integration of equation 3.1 yields

$$n(t) = n_0 e^{-\alpha t} \quad (3.2)$$

where n_0 is the neutron density at $t = 0$ and

$$\alpha = \frac{\beta - \rho}{\Lambda} \quad (3.3)$$

When the reactor is exactly critical $\rho = 0$ which results in the Rossi Alpha.

$$\alpha_0 = \frac{\beta}{l} \quad (3.4)$$

However, the total neutron density in a reactor is composed of source and delayed neutrons in addition to the prompt neutrons indicated by equation 3.2. The total neutron density is

$$n_T(t) = n_0 e^{-\alpha t} + n_B \quad (3.5)$$

where n_B represents source and delayed neutron contributions which are statistically uncorrelated in their time behavior.

This equation represents the total neutron density within a point reactor at any instant.

Counts accumulated in a multichannel analyzer result from an integration of the instantaneous count rate over the channel width.

$$N_T = \int_{t_1}^{t_2} n_T dt \quad (3.6)$$

$$N_T = \int_{t_1}^{t_2} n_0 e^{-\alpha t} dt + \int_{t_1}^{t_2} n_B dt \quad (3.7)$$

Defining t_{ch} as the channel width one finds

$$t_1 = t_2 - t_{ch}$$

and then, after integration and rearrangement,

$$N_T = \frac{n_0 (e^{\alpha t_{ch}} - 1)}{\alpha} e^{-\alpha t_2} + n_B t_{ch} \quad (3.8)$$

For any given reactor configuration, n_0 , α , and t_{ch} are constants. Therefore, a plot of $\ln (N_T - n_B t_{ch})$ vs. t_2 should yield a line having a slope of $-\alpha$. The intercept of this line is

$$\ln \left[\frac{n_0 (e^{\alpha t_{ch}} - 1)}{\alpha} \right] \quad (3.9)$$

Babala [3] discusses the significance of this intercept for the Rossi Alpha Method and Orndoff's [17] experiment.

A relationship between the prompt neutron decay constant and the uncorrelated background count may also be derived. For a subcritical reactor at equilibrium in the presence of a neutron source, the following situation exists:

$$\frac{dn}{dt} = 0 = \frac{\rho - \beta}{\Lambda} n_s + \lambda C_s + S \quad (3.10)$$

$$\frac{dC}{dt} = 0 = \frac{\beta}{\Lambda} n_s - \lambda C_s \quad (3.11)$$

where S is the source rate and the subscript s refers to the steady state values.

From equation 3.11

$$C_s = \frac{\beta k n_s}{\lambda \ell} \quad (3.12)$$

$$C_s = \frac{\alpha_0 k n_s}{\lambda}$$

Equations 3.10 and 3.12 yield:

$$\alpha = k \alpha_0 + S/n_s \quad (3.13)$$

$$\alpha \approx \alpha_0 + S/n_s \quad (3.14)$$

(for $k \approx 1$)

A plot of α as a function of $1/n_s$ should yield an intercept at α_0 , the Rossi Alpha. If the average counting rate of a detector is assumed to be proportional to n_s , then

$$\alpha = \alpha_0 + \frac{K}{c} \quad (3.15)$$

where c is the average count rate and K is a proportionality constant.

From the definitions of α and α_0 a relationship between prompt neutron decay constant and the degree of reactor subcriticality can be derived.

$$\frac{\rho}{\beta} = 1 - \frac{\alpha}{k \alpha_0}$$

$$\rho(\$) \approx 1 - \frac{\alpha}{\alpha_0} \quad (3.16)$$

(for $k \approx 1$)

where: $\rho(\$) = \rho/\beta =$ reactivity in dollars

Bierman et al. [4] defined the following expression as a figure of merit for decay experiments in the presence of background events.

$$\eta = \frac{n_0}{n_0 + n_B} \quad (3.17)$$

The value n_0 is shown by Babala [3] and Thie [22] to be primarily dependent upon the number of neutrons released per fission, ν , and is therefore invariant with respect to reactor power. The dependence of n_0 on prompt multiplication constant does result in some sensitivity towards reactivity but this effect is minor since changes in reactivity during this experiment result in at most a 2 percent change in multiplication factor.

The value of n_B is directly related to reactor power and therefore the value of η decreases for increasing power levels. Clearly, a relatively large value for η is desired as this will result in the exponential term dominating equations 3.5 and 3.8, thereby decreasing the sensitivity of the experiment to the uncorrelated neutron detections. Obviously low reactor power levels are preferred. Pacilio [18] claims that it becomes impractical to attempt prompt neutron decay experiments when the uncorrelated component exceeds 0.2 neutrons per prompt neutron lifetime (approximately 2000 counts per second for thermal systems).

Measurement of decay constants based on variance to mean determinations are shown by Thie [22] to be represented by the following equation:

$$\frac{\overline{c^2} - (\bar{c})^2}{\bar{c}} = 1 + Z \left[1 - \frac{1 - e^{-\alpha\tau}}{\alpha\tau} \right] \quad (3.18)$$

where

c_i = counts accumulated in channel i

$$\bar{c} = \frac{1}{N_{ch}} \sum_{i=1}^{N_{ch}} c_i$$

$$\overline{c^2} = \frac{1}{N_{ch}} \sum_{i=1}^{N_{ch}} c_i^2$$

N_{ch} = number of channels

τ = gate time (channel width)

The constant Z is dependent upon ν , β , ρ and the detector efficiency ϵ which is defined as the number of counts registered per fission event.

Data for this type of analysis are obtained by making a single scan of approximately 1000 sequential channels at a gate time τ . The scan may occur at any time and is not initiated in response to a trigger neutron detection. Scans for approximately ten to twenty different gate times are made with the resulting variance to mean ratios being fit to equation 3.18 as a function of the gate time. For thermal reactors gate times of between 500 μ s and 100ms are usually

employed. Fitting the data to equation 3.18 may be accomplished using a chi-square criterion.

Reflected cores are characterized by the presence of two exponentials [2]

$$n_t = n_B + Be^{-\alpha t} + Ae^{-\alpha' t} \quad (3.19)$$

where the constants B and A are the components of n_0 which characterize an unreflected and reflected core respectively. The value of α' is associated with neutrons which have spent time in the reflector before being returned to the core to cause another fission event. The result of this process is to effectively increase the neutron lifetime and therefore the prompt neutron decay constant, α' , associated with the reflector is smaller than the decay constant, α , attributed to the core composition.

B. Data Collection Methods

A flowsheet for a data acquisition-data reduction system based on the Rossi Alpha Method is shown in Figure 3.1. The number of channels, channel widths, and number of channel scans are input in response to a request prompted by the computer. Data are then collected in accordance with these parameters and output to a terminal which allows the operator to decide whether the counts accumulated are sufficient to be statistically significant. If not, more data can be accumulated. If the data are sufficient, the computer can make a least squares fit to determine α . After several values of α are obtained, the value of α_0 and reactivities associated with each of the reactor configurations are calculated.

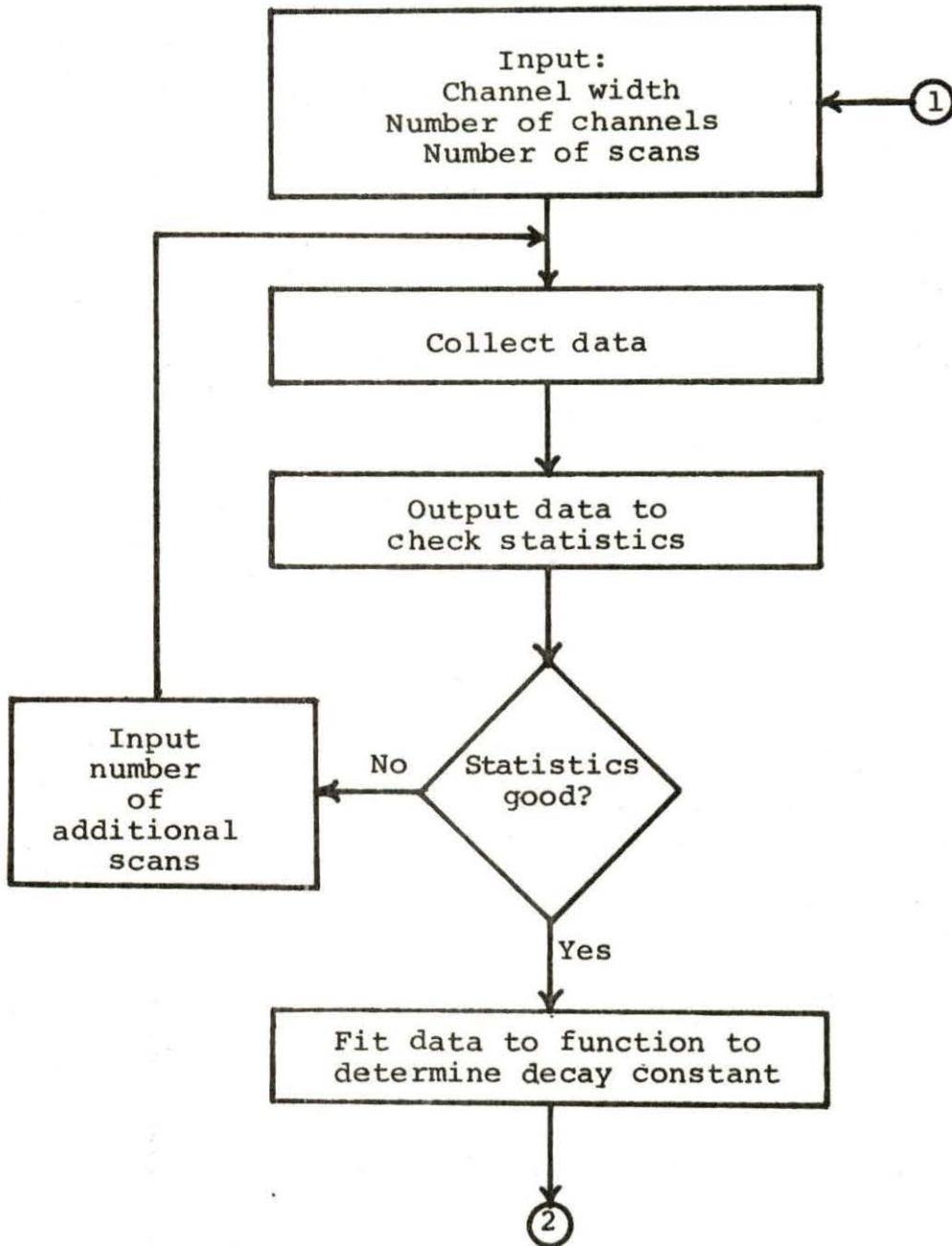


Figure 3.1. Consolidated acquisition-analysis program based on the Rossi Alpha Method

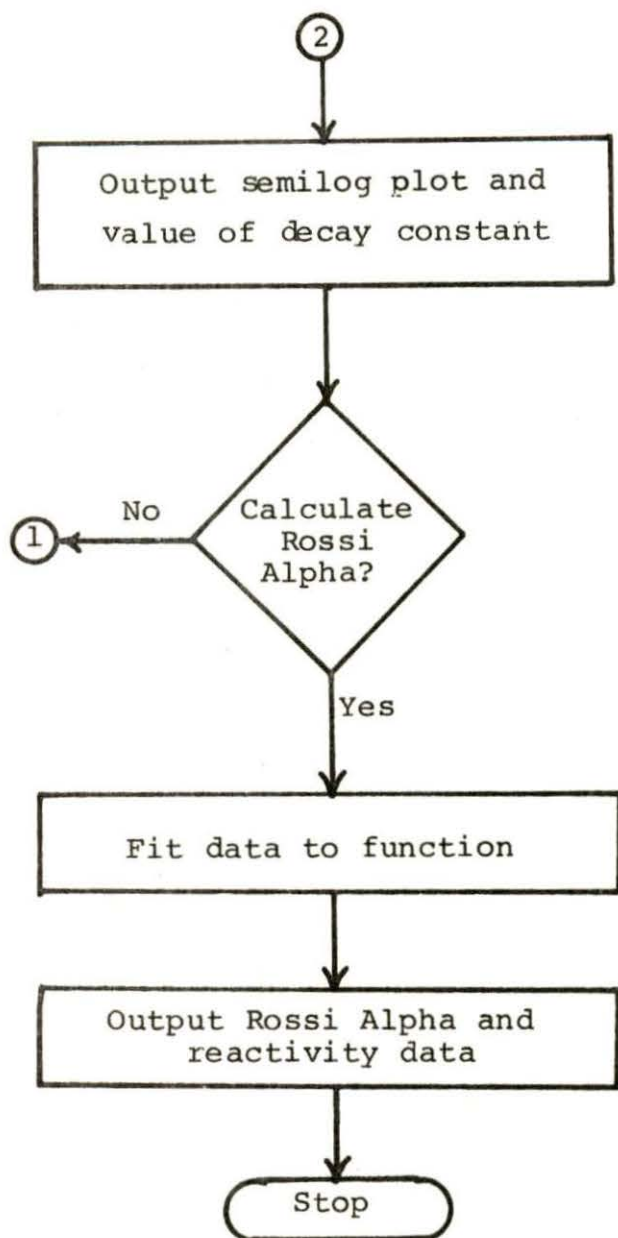


Figure 3.1 continued

Figure 3.2 shows a data acquisition-data reduction scheme based on a variance to mean type of analysis. The number of gate widths and values for each of the gate widths are input to the computer. Data for each of the gate widths are collected and the variance to mean ratio determined. After fitting the data to equation 3.18 to determine the prompt neutron decay constant, a new reactor configuration can be requested by the computer. Either the variance to mean analysis is performed at a new reactor configuration or, if a sufficient number of decay constants have been collected, the Rossi Alpha for the reactor and degree of subcriticality for each reactor configuration can be calculated.

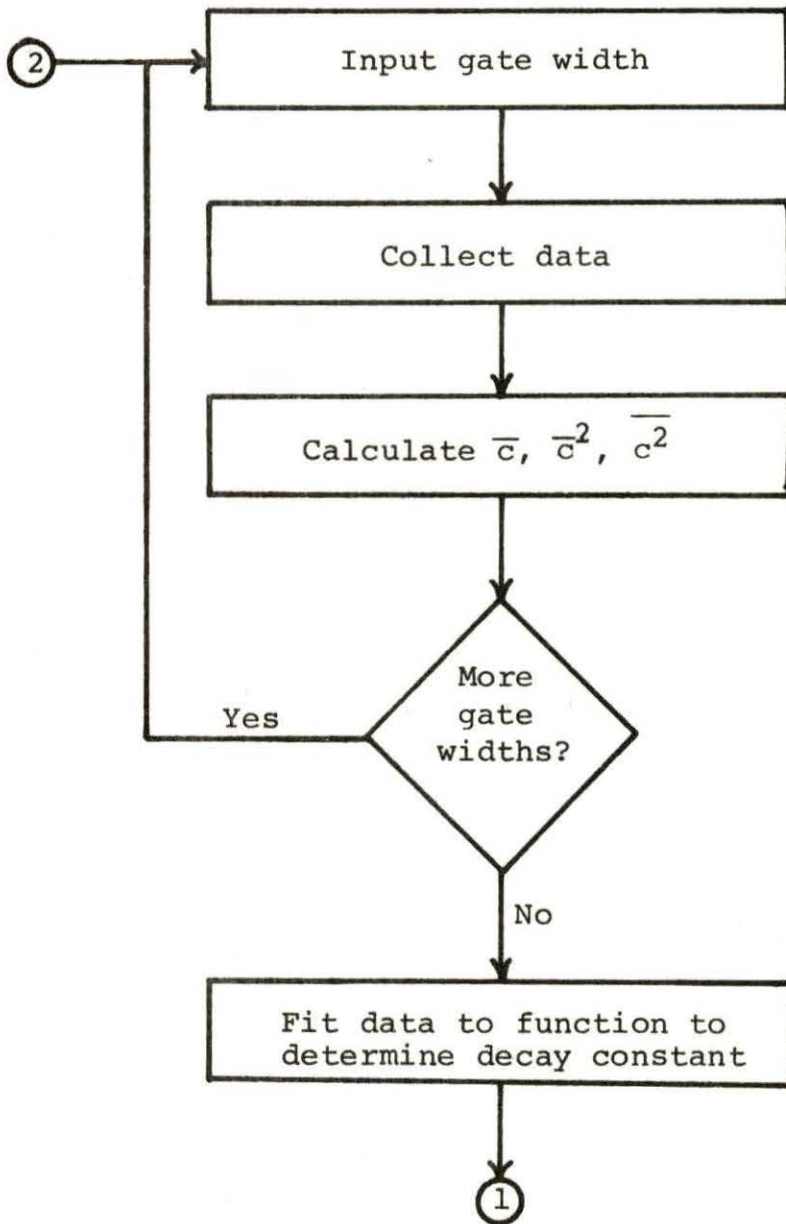


Figure 3.2. Consolidated acquisition-analysis program based on a variance to mean approach

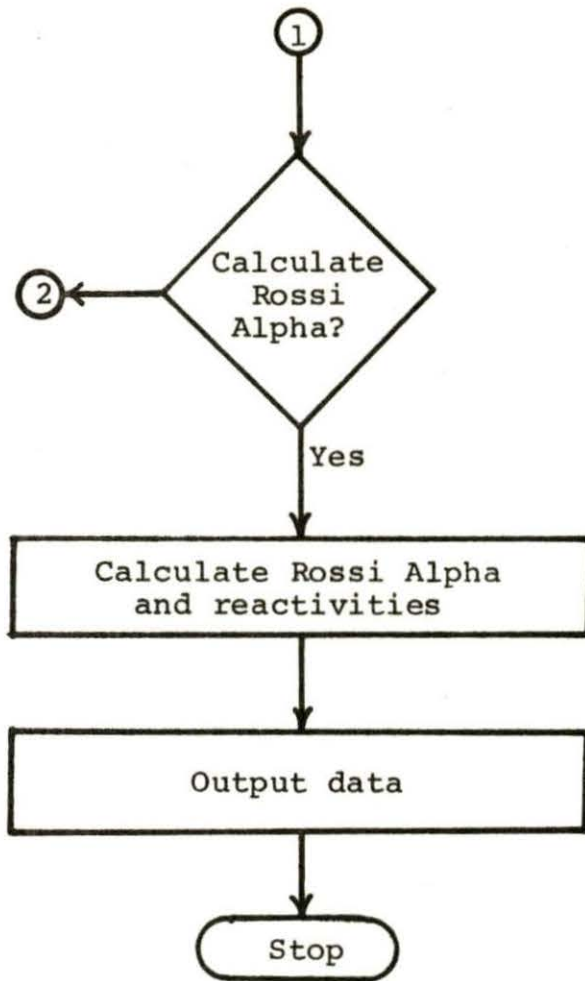


Figure 3.2 continued

IV. EXPERIMENT

A. Data Acquisition System

A block diagram of the KIM-1 microcomputer is shown in Figure 4.1. The central processor unit is a MOS 6502 microprocessor. The two peripheral interface adaptors (6530-002 and 6530-003) contain a monitor program which supervises some basic KIM-1 operations in addition to providing the capability to interface with external peripheral devices. Examination of Figure 4.1 reveals that PIA 6530-002 is dedicated to the hexadecimal keyboard, light emitting diode display and teletype interface. The other PIA, 6530-003, is available for interfacing with external devices to allow information transfer from an experiment to the microcomputer. Soucek [21] presents the basics for general microcomputer operation while a detailed description of the KIM-1 system may be found in reference [14].

The relatively small amount of memory available on the KIM-1 microcomputer places severe restrictions on the size and complexity of programs which may be implemented. Routines which require multiplication and division consume large amounts of the available memory on the KIM-1. As a result, no attempt was made to synthesize a complete data acquisition-data reduction system based on this microcomputer. Other larger microcomputers equipped with a high level language such

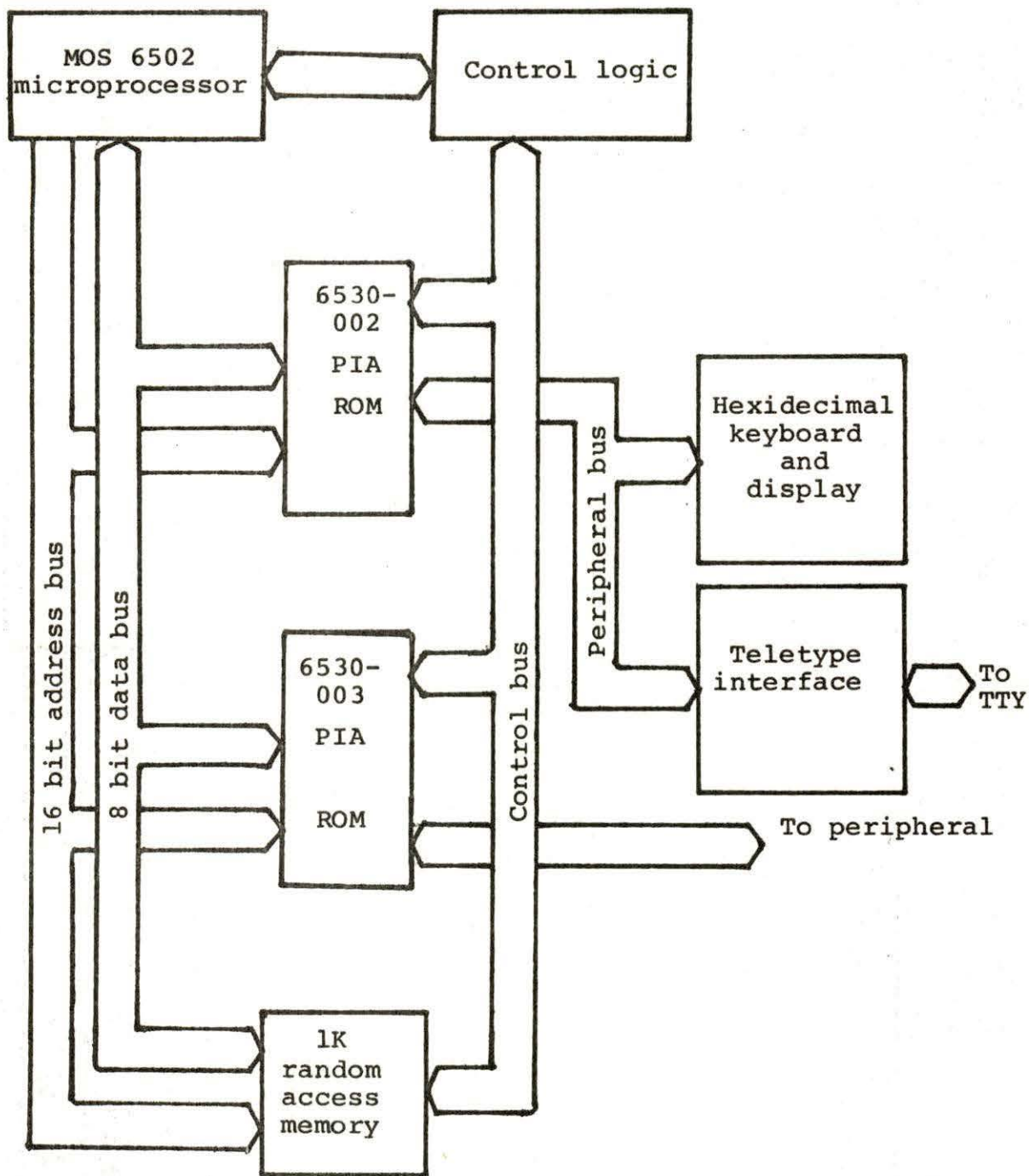


Figure 4.1. KIM-1 microcomputer

as BASIC are more amenable to the task of data reduction. Communication with the data collection routine, which would most likely be stored in machine code on a read-only memory, would be accomplished through the "PEEK", "POKE", and "USER" commands included in the instruction set of the higher level language. The KIM-1 system to be described was used as a data acquisition device only, with all calculations and curve fittings being performed externally.

The following three factors were the primary considerations in developing the microprocessor-based data acquisition system:

1. Dead times of less than $1\mu\text{s}$ between each channel.
2. Minimum dead time between the detection of the trigger neutron and initiation of the channel scan.
3. Stable and reproducible channel widths.

In order to minimize channel dead times, two 4-bit BCD counters were employed. This arrangement allows one counter to collect data while the data from the other counter are being stored. Channel dead times are estimated to be less than one machine cycle (i.e. $1\mu\text{s}$). An external timer is included in the design to provide a minimum channel width. Changing the channel width is accomplished by creating a variable length loop in software. An in-depth description of the counter-timer peripheral appears in Appendix A. A block diagram of the complete data acquisition system is presented

in Figure 4.2. The components of this system are as follows:

1. High voltage power supply, Fluke Model 412B.
2. Proportional preamplifier, Canberra Model 806.
3. Spectroscopy amplifier, Canberra Model 816.
4. Single channel analyzer, Canberra Model 830.
5. Scaler, Canberra Model 873.

The selection of a detector and the actual settings of these components will be discussed in a subsequent section.

A flowsheet of the data collection routine ROSSI.SRC is shown in Figure 4.3. Two points exist for entry into the program. Entry point 1 is used when an entirely new set of data is desired, as this includes a routine to zero the segment of memory corresponding to the data channels. Entry point 2 is used if more data at the same reactor configuration are to be accumulated. For example, this may occur after examining the channel contents and finding that insufficient counts were accumulated to yield statistically significant results. Restarting the data collection routine at point 2 will allow accumulation of additional counts without having to repeat scans which are already present.

The system initialization step defines which bits on PIA 6530-003 are to be used for control lines and which are to be used as data input lines. After the counters are cleared, counter 1 is enabled and the contents of counter 1 are

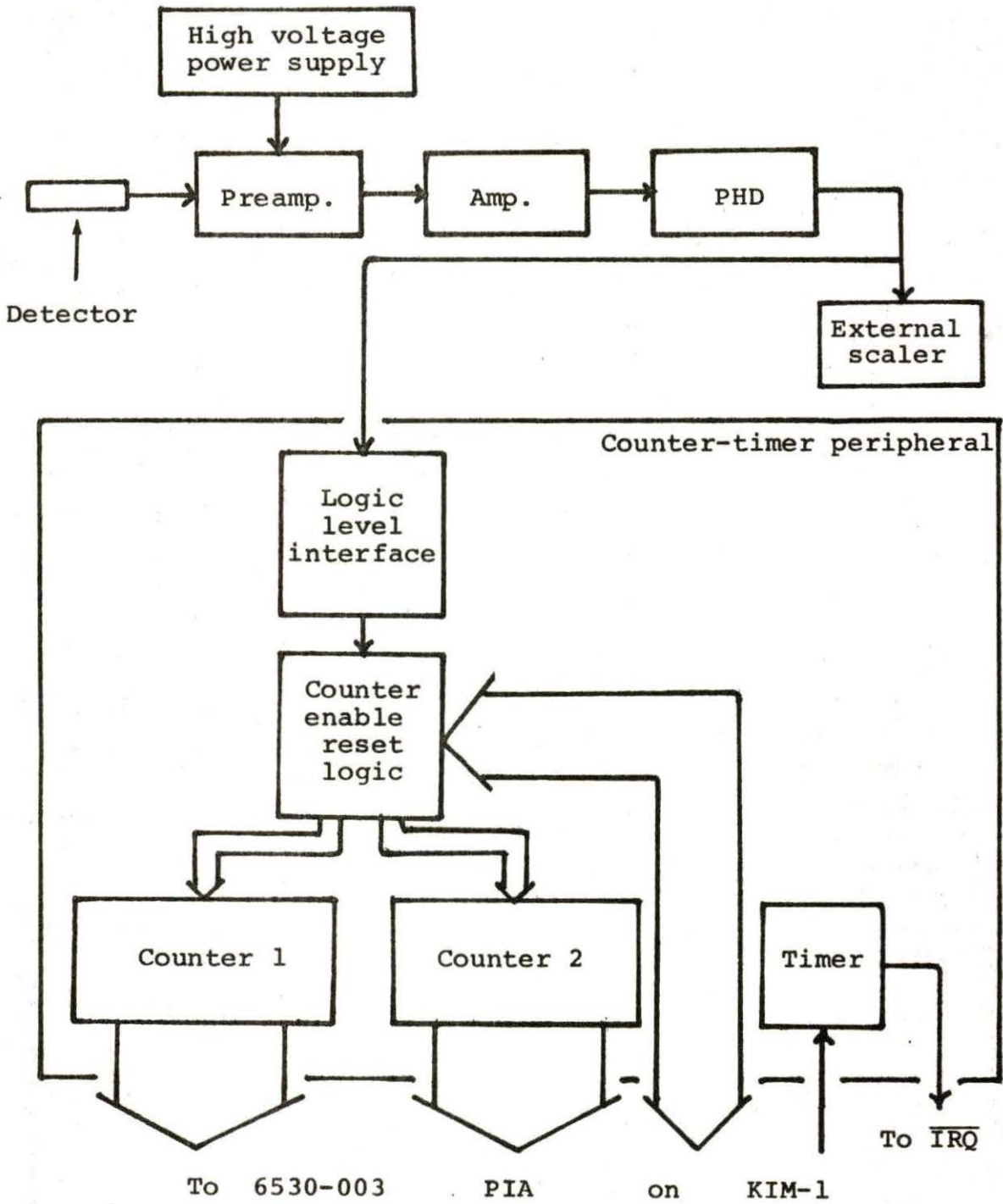


Figure 4.2. Data acquisition system

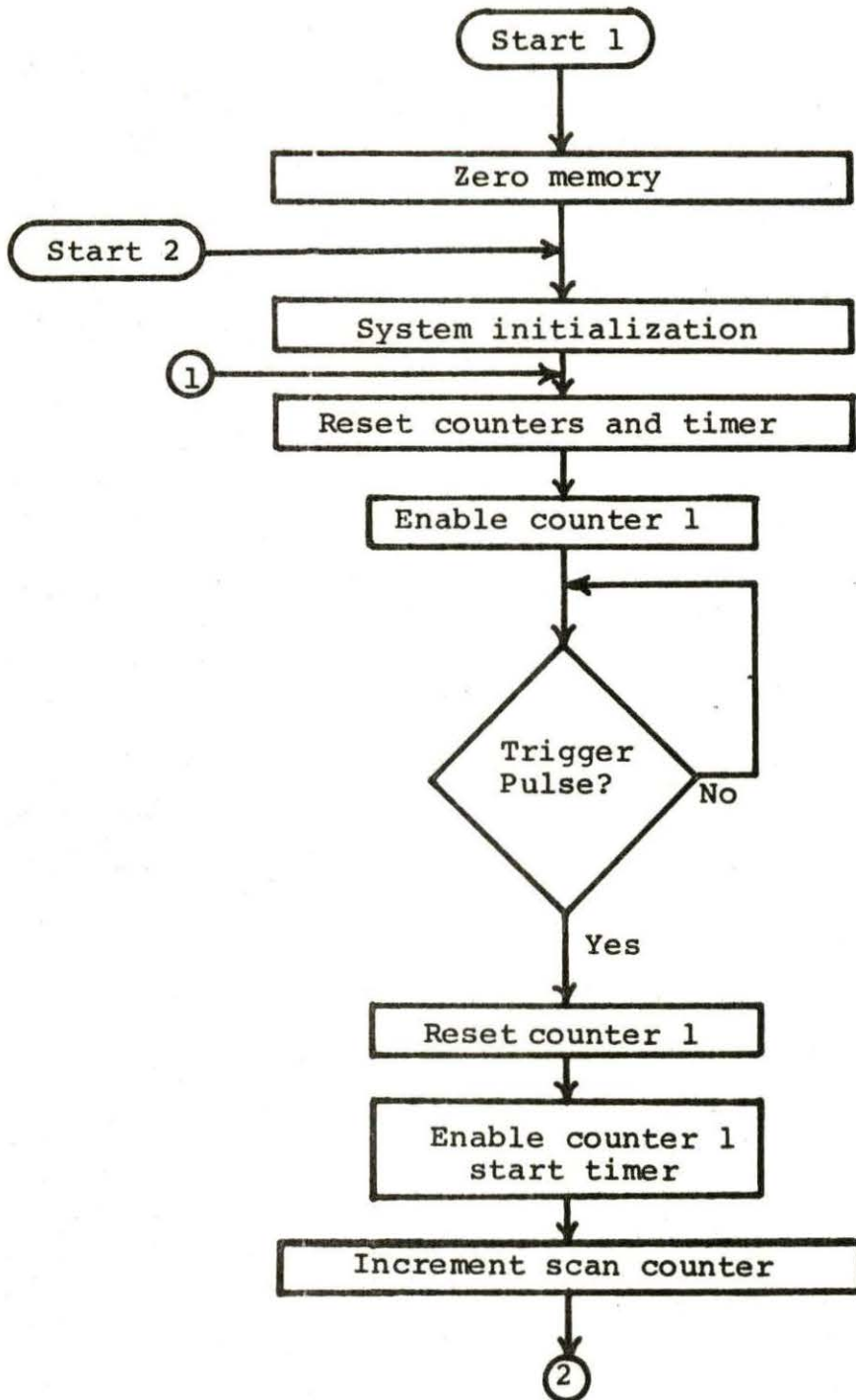


Figure 4.3. Flowsheet for data collection routine ROSSI.SRC

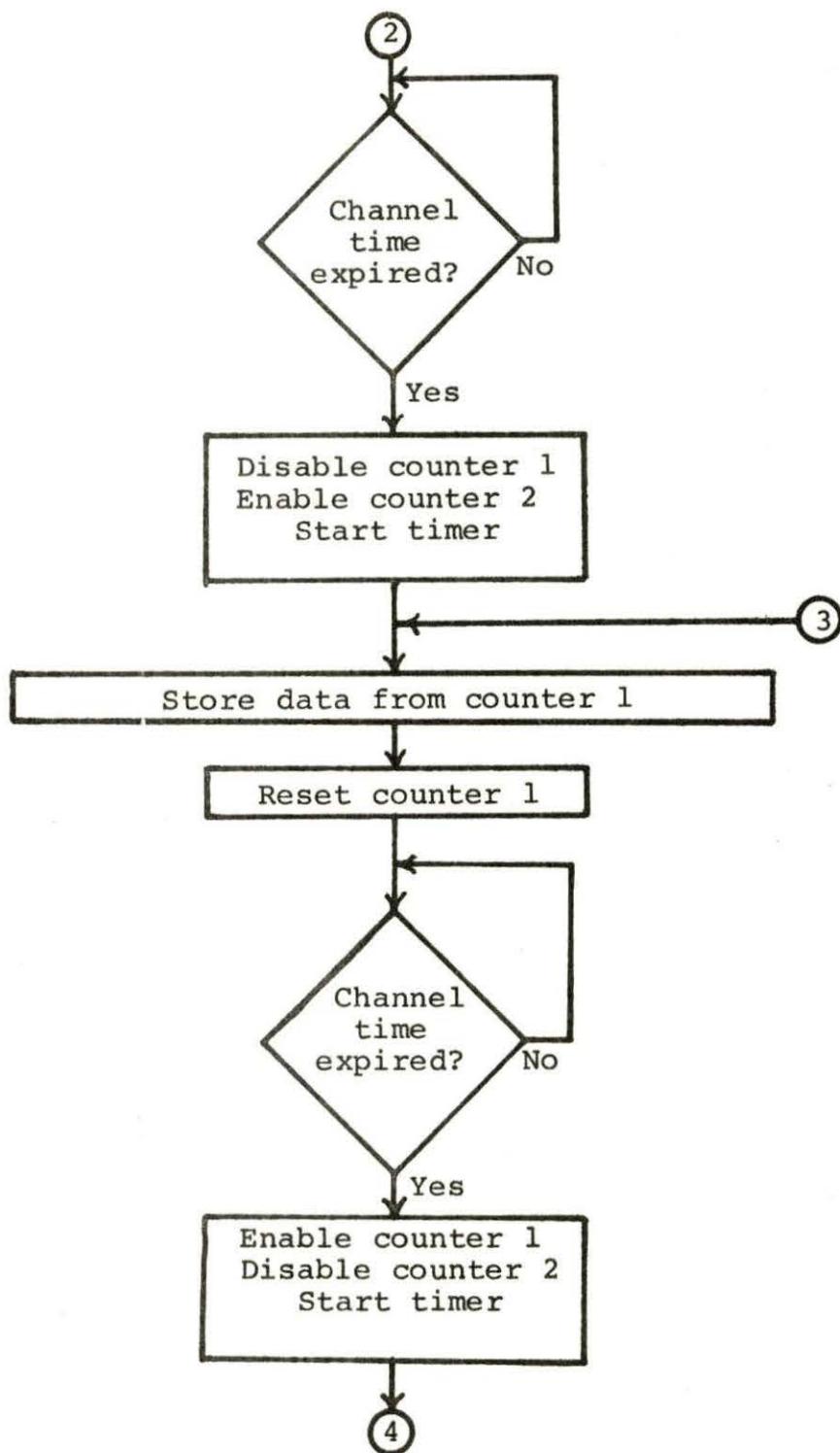


Figure 4.3 continued

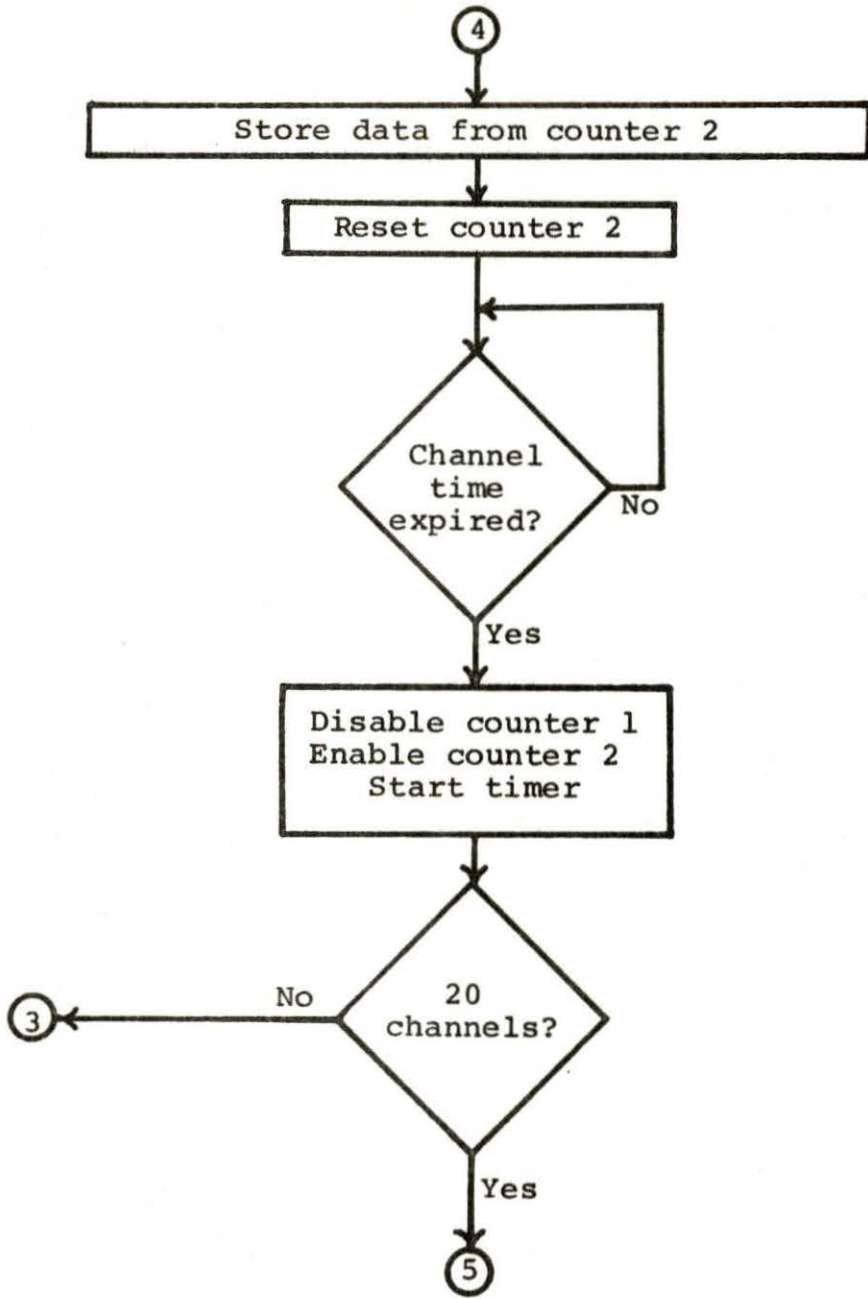


Figure 4.3 continued

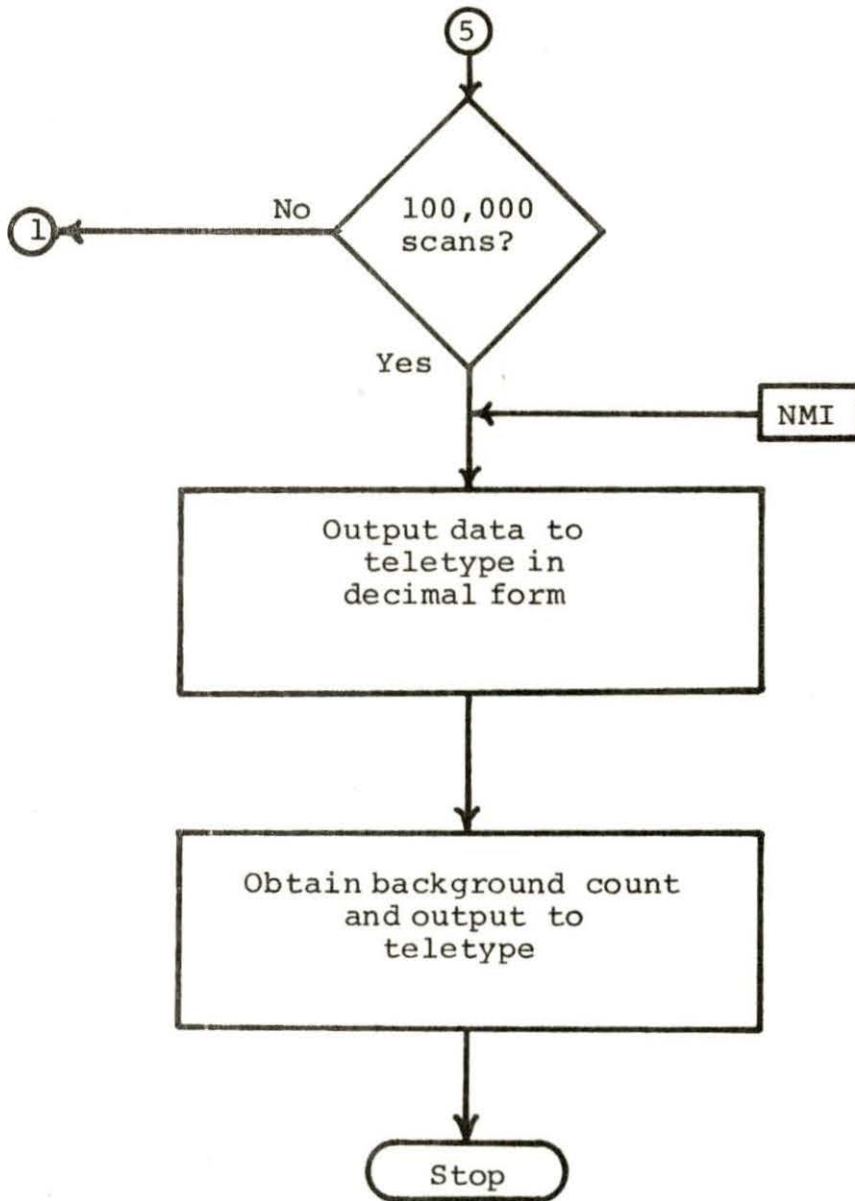


Figure 4.3 continued

examined in a loop. If the value of this counter exceeds zero, corresponding to the detection of a trigger neutron, the program branches out of the loop and begins a scan of twenty sequential channels. This approach results in a dead time which varies from $14\mu\text{s}$ to $20\mu\text{s}$ between the detection of a trigger neutron and initiation of the channel scan sequence.

After one-hundred thousand triggered scans, the data accumulated in the twenty channels is output to the teletype. Data output may be obtained at any time by executing a non-maskable interrupt.

Immediately following the output routine a background count is obtained based on the number of triggered scans previously used. The results of the background measurement are then output to the teletype.

A description of routine ROSSI.SRC may be found in Appendix C. A data collection routine based on the variance to mean type of analysis is described in Appendix D. Although the latter method was not applied during the course of this investigation, it is presented as a possible basis for further work.

B. Selection of Detector and Optimum Operating Parameters

The success of a prompt neutron decay experiment is primarily influenced by the following four factors:

1. Channel width.
2. Number of channels used.
3. Detector efficiency.
4. Geometry of the system.

The choice of channel width determines the resolution of the experiment and therefore, is based on the value of the prompt neutron decay constant. Channel width is determined by the value of a hexadecimal constant stored at memory location \$02FA. A ^3He detector used in conjunction with a Pu-Be source to supply random counting events to the data acquisition system, provided channel width calibrations for several constants stored at \$02FA. The results of this calibration are shown in Figure 4.4. The channel widths represent an average over twenty channels. The width of an individual channel is expected to vary approximately $\pm 5\mu\text{s}$ depending on when the interrupt request signal is received from the external timer. This is explained in greater detail in Appendix C. This variation is assumed to be random and therefore, in the limit of an infinite number of scans each individual channel width should be equal to the mean. A plot of percent channel width deviation as a function of channel number for an expected mean channel width of $497\mu\text{s}$ is shown in Figure 4.5. These values were obtained using a random source (Pu - Be) with a detection rate of 1540 ± 4 counts/s and were obtained by averaging over 240,000 scans of

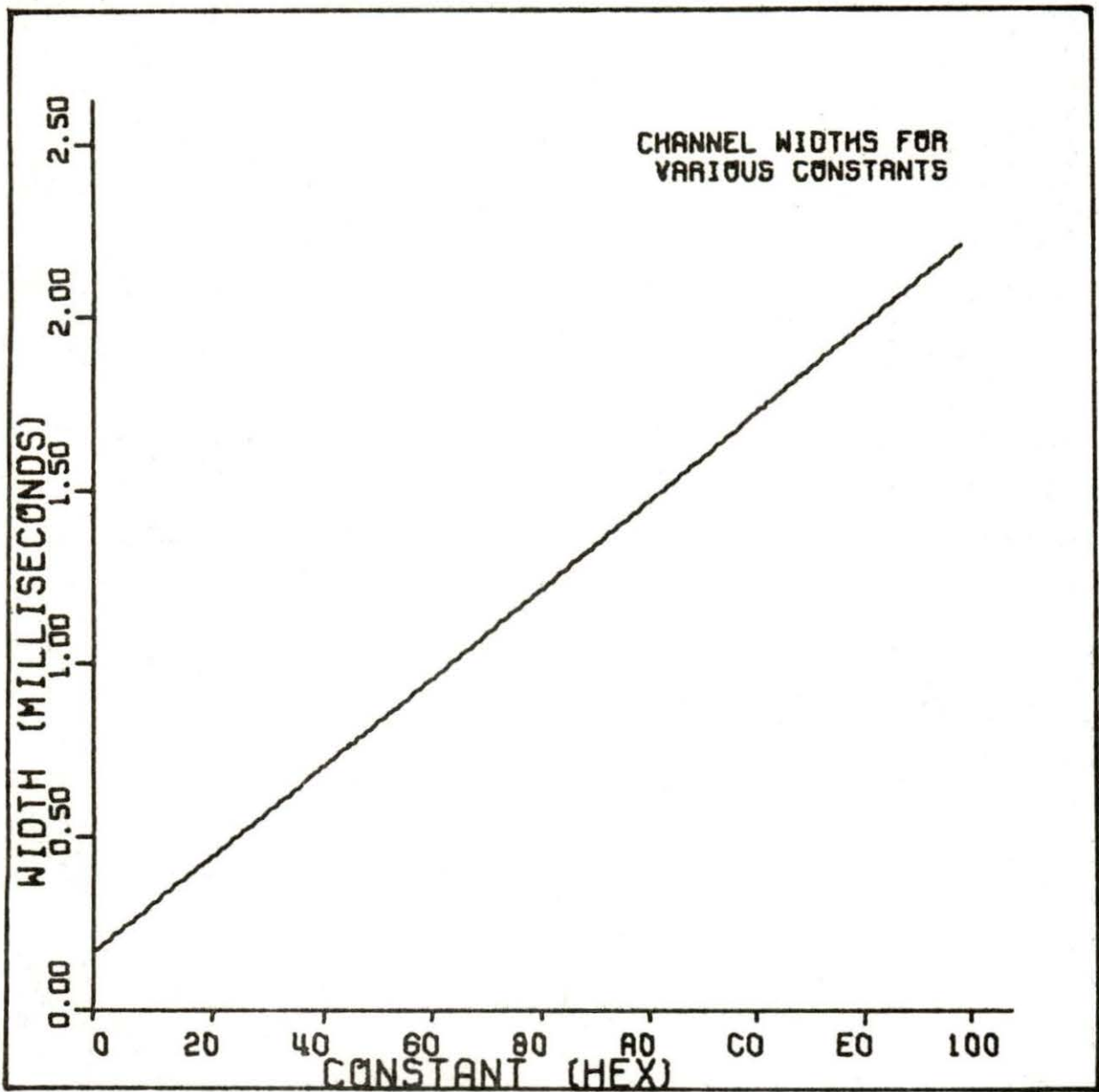


Figure 4.4. Channel width for various hexadecimal constants stored in timer routine

each channel. An error of ± 0.2 percent may be attributed to the statistical deviation of the source count rate, assuming that the source rate does not vary by more than one standard deviation. Inspection of Figure 4.5 reveals that many of the channel width deviations exceed the expected 0.2 percent. This result indicates that the assumption that errors resulting from the timing of the interrupt request signal will cancel for a large number of scans may not be entirely correct and is questionable for the number of scans used here. No explanation can be offered for the extreme deviation from the mean for channel 1, therefore this channel was not included in the data analysis.

Prompt neutron decay measurements using a ^3He detector located as close to the fuel as possible, were conducted with channel widths of $176\mu\text{s}$, $296\mu\text{s}$, $497\mu\text{s}$, $615\mu\text{s}$ and $1060\mu\text{s}$, in order to determine an optimum value for the channel width. The results of these studies indicated that long data collection times (many triggered scans) were necessary to obtain a statistically significant number of counts in each channel. This reduced scatter resulting from the random nature of the uncorrelated neutron detections. Also, the exponential decay was observable for all of the channel widths employed. These measurements indicated that the prompt neutron decay constant with all control rods inserted was in the range of 160 rad./s to 190 rad./s .

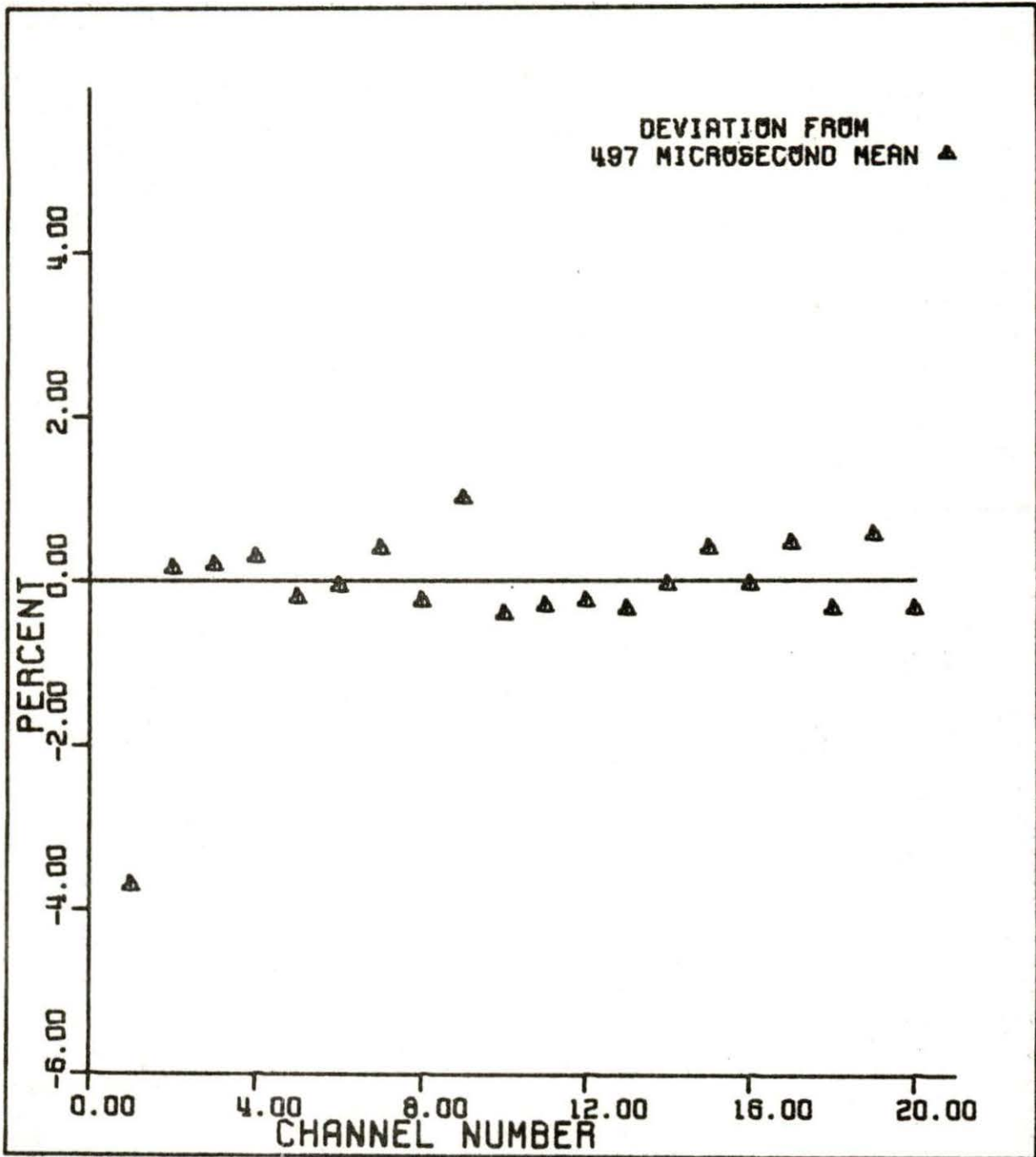


Figure 4.5. Microcomputer channel width deviation

A total of sixty channels was used for each measurement as a means of determining how far into the exponential decay the scan should extend. It was found that for times greater than $2/\alpha$ the data were essentially at the background value. Accumulating data for times greater than $2/\alpha$ results in sending negative arguments to logarithmic functions in the computer code used for data analysis due to the statistical variation of the background count.

For practical purposes it is necessary to minimize the data collection time at each reactor configuration. It is possible to derive an equation to calculate the time required for making N channel scans.

The time required to scan through the channels following an initial trigger neutron detection is simply $t_{ch}N_{ch}$, where N_{ch} is the number of channels. Before the next scan can be undertaken, the program must cycle back to the trigger detection loop. The time required to accomplish this is t_{cyc} . Next, the program must wait for t_w seconds until a neutron is detected to trigger the scan sequence. The total amount of time required for each scan cycle is given by:

$$t_T = t_{ch}N_{ch} + t_{cyc} + t_w \quad (4.1)$$

If these times are in seconds, the total time, t_{coll} (in minutes), required to make N channel scans is

$$t_{coll} = \frac{N(t_{ch}N_{ch} + t_{cyc} + t_w)}{60}. \quad (4.2)$$

Since $t_{ch} N_{ch}$ is equal to the amount of time data are taken from the exponential decay, an upper limit for this value may be determined. If the maximum value of α expected for these experiments does not exceed 200 radians/s, for example, then

$$t_{ch} N_{ch} = 2/\alpha = 10\text{ms} .$$

The value of t_{cyc} was empirically determined to be approximately 3ms. The value of t_w can be approximated by $t_w = 1/(\text{mean count rate})$. Equation 4.2 becomes:

$$t_{coll} = \frac{N}{60} \left[0.013 + (\text{mean count rate})^{-1} \right]. \quad (4.3)$$

Initially it may not appear that the data collection time is dependent upon the channel width. However, if the counting statistics for various channel widths are to remain the same, the number of triggered scans, N , will have to increase for decreasing channel widths. By way of example, if the length of time each channel is allowed to collect data is to remain constant, a channel width of $176\mu\text{s}$ would require approximately six times the number of scans compared to a channel width of $1060\mu\text{s}$. Since the value of reciprocal mean count rate ranged from 0.0015s to 0.02s, channel width becomes an important consideration.

Based on the channel widths available, number of data points required for a least-squares fit, expected range of prompt neutron decay constants, and what was considered to be a

reasonable data collection time, a total of 20 channels having an average width of $497\mu\text{s}$ was chosen.

Although the deviation in channel width was larger than was desired (± 1 percent, neglecting channel 1), it was a considerable improvement in comparison to the available multiscalers (± 3 percent). Other improvements realized were the reduction in channel dead times from approximately $10\mu\text{s}$ to less than $1\mu\text{s}$ and a reduction in data collection time due to the greater flexibility in choosing the channel width and number of channels to be scanned. The dead time between the detection of a trigger neutron and initiation of the channel scan sequence was increased several microseconds by using the KIM-1 microcomputer. A modification which could reduce this dead time and the channel width deviation is presented in Appendix C.

A drawing of the core region of the UTR-10, a water-moderated, graphite-reflected, coupled-core reactor, is shown in Figure 4.6. Each core tank contains approximately 1.5 kg of 93 percent enriched uranium. A penetration in the reflector allows for detector placement within 11cm of the south core.

Mounting a detector inside one of the cores was impractical primarily due to the reactor operations schedule. Therefore, both graphite stringers were removed from the thermal column and detectors for the experiment were placed as close to the south core as possible.

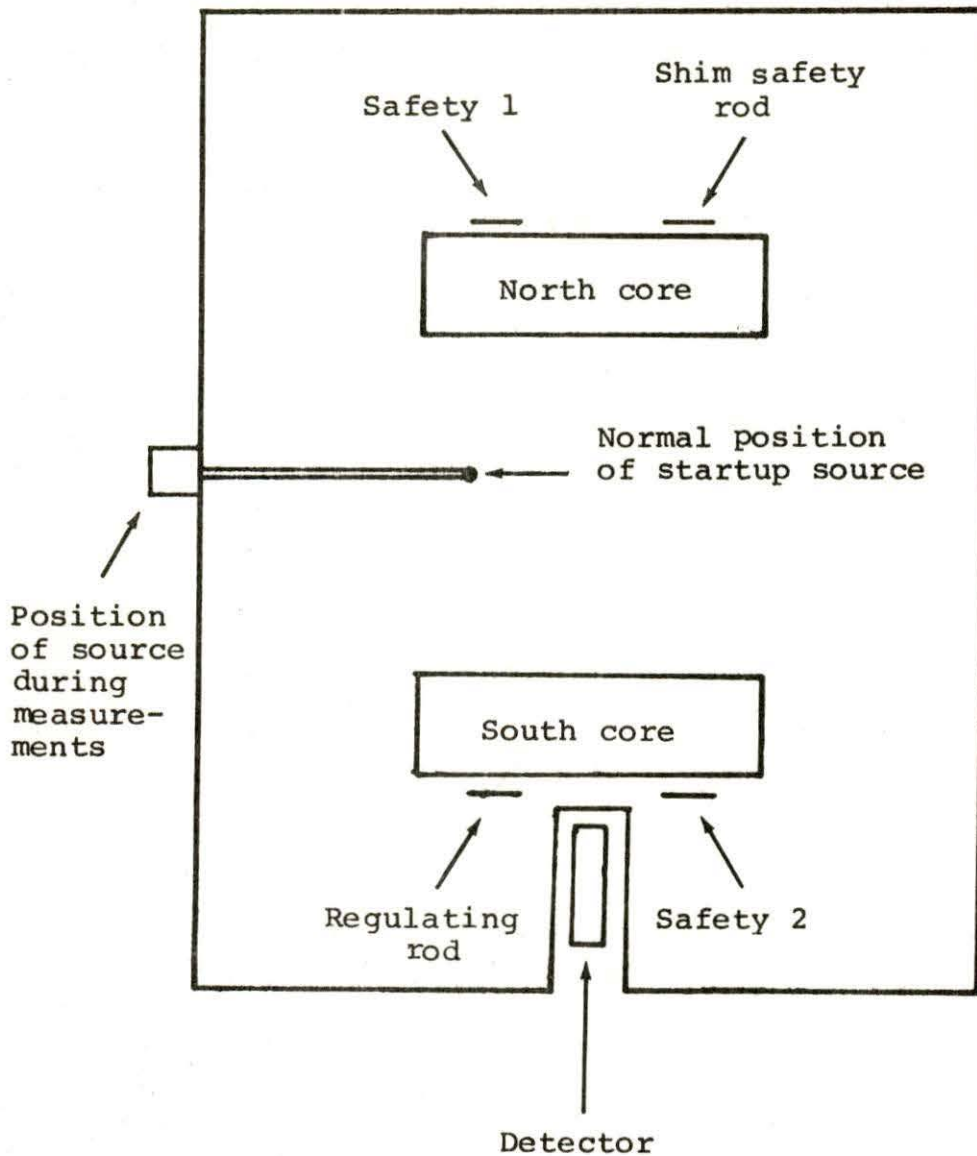


Figure 4.6. Geometrical arrangement of the UTR-10 coupled core reactor

Three types of neutron detectors were examined for use in this experiment— ^3He , BF_3 , and a fission chamber. The spectral response of the ^3He and BF_3 detectors to thermal neutrons and gammas are shown in Figure 4.7. The large number of counts obtained at small MCA channel numbers result from the response of the detectors to gammas. The shape of the response curves for both detectors are very similar and although the ^3He detector has a greater sensitivity for neutrons, the BF_3 detector exhibits a greater sensitivity for gammas. The similarity of the two spectra implies that a single pulse height discriminator setting may be used for either detector. The window of the single channel analyzer was opened to 100 percent, and the discriminator setting rejected signals occurring below channel 100 in the spectra. This provided ample discrimination against the gamma background.

A plot of the figure of merit, as defined by equation 3.17, for the various detector schemes investigated is presented in Figure 4.8. The reactor configuration during these measurements had both safety rods fully withdrawn (reactor approximately \$0.50 subcritical). If the mean count rate is an index of sensitivity, the ^3He detector is the most sensitive, but it also exhibits the lowest figure of merit. In an attempt to improve the figure of merit, a cadmium cylinder, open on each end, was placed around the detector.

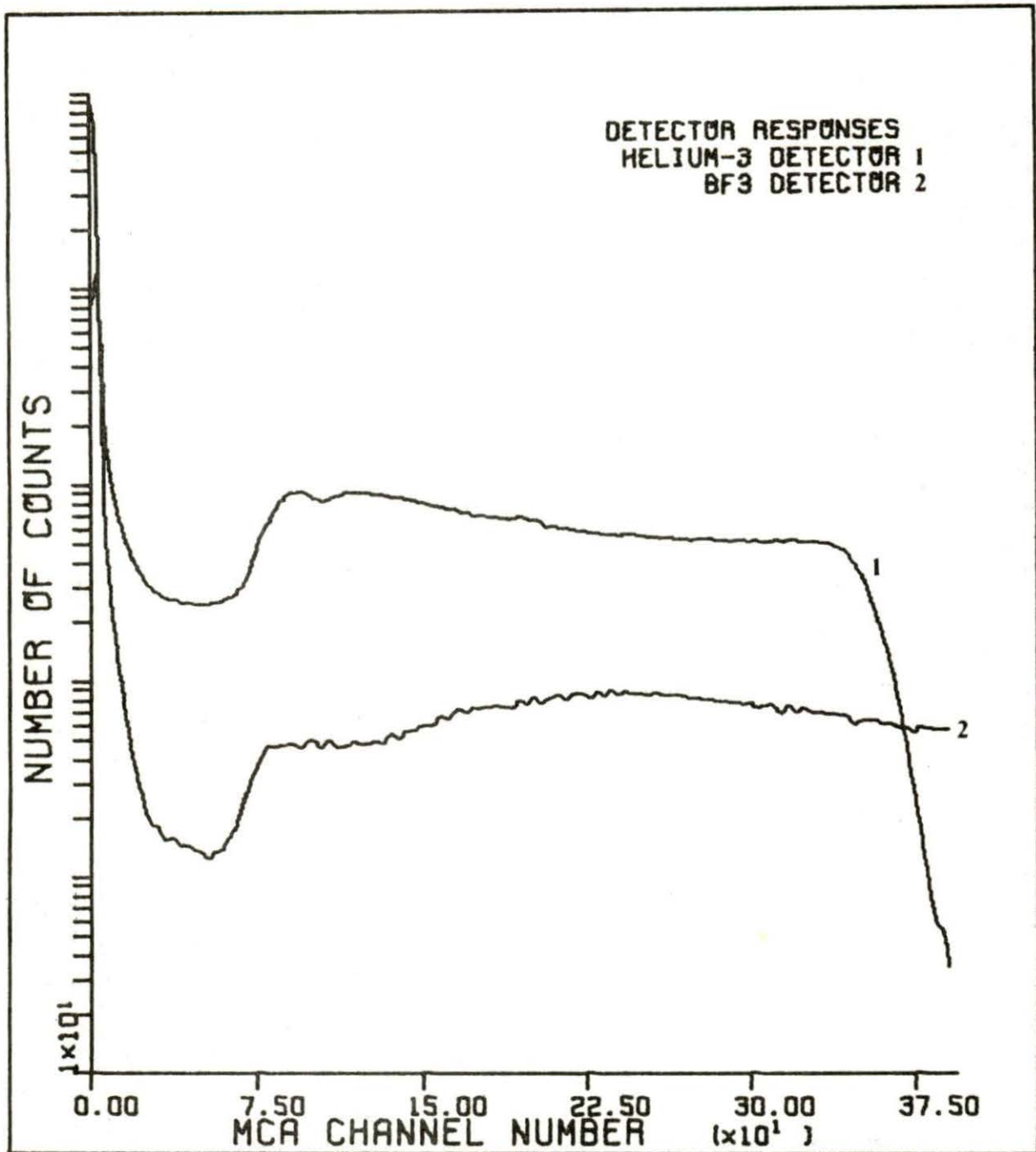


Figure 4.7. Response of ^3He and BF_3 detectors to thermal neutrons and gammas

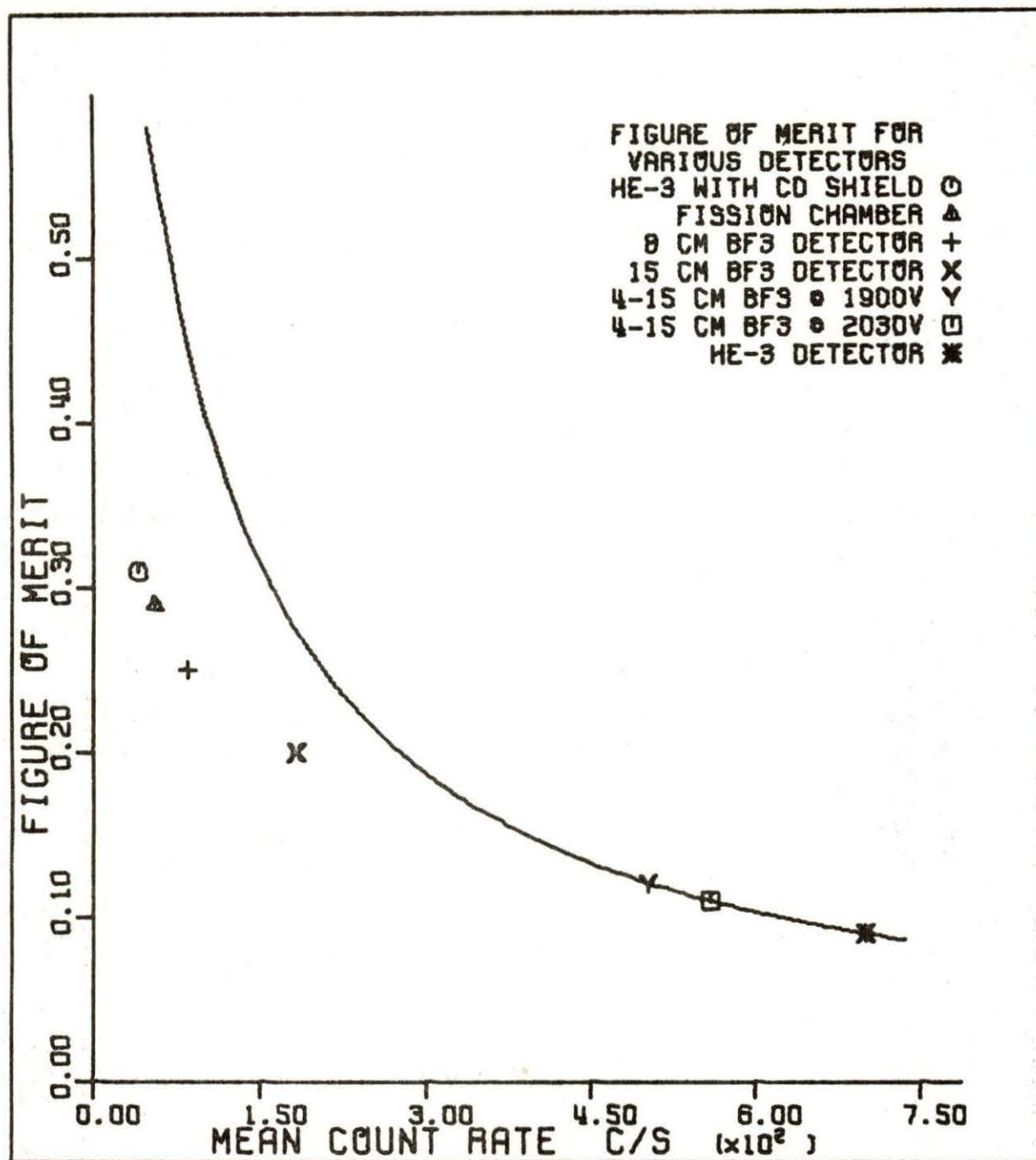


Figure 4.8. Figure of merit for various detector arrangements

The background count was reduced by shielding against uncorrelated thermal neutrons which were entering the detector. Neutrons reaching the detector soon after a fission event were assumed to have energies greater than 0.4eV (the cutoff energy for cadmium) in order to be well-correlated to a particular fission chain. Thus, the value of n_B was to be reduced by geometrical arrangement and cadmium shielding, while n_0 was to be only slightly effected primarily due to neutron spectrum considerations. Figure 4.8 shows that this situation did yield the largest figure of merit for all of the detector schemes tried. The curve representing equation 3.17, based on the figure of merit for the unshielded ^3He detector, is shown in Figure 4.8 and predicts a much larger figure of merit than was actually obtained. Apparently a significant decrease in the value of n_0 also resulted from the addition of the cadmium shield.

Other detector schemes tried were: an 8cm long BF_3 detector, a 15cm long BF_3 detector, clusters of four 15cm long BF_3 detectors at 1900 volts and 2030 volts, and finally a fission chamber. Clearly all the points lie on a smooth curve which is below the curve representing equation 3.17. If the mean counting rate is used as an index of detector sensitivity, the values of n_0 and n_B are not effected equally by changes in sensitivity. If they were the figure of merit would remain constant. Low detector sensitivities favor

the exponential term of equation 3.8. Unfortunately low detector sensitivities lead to extremely long data collection time requirements. Based on 100,000 scans of twenty channels with an average width of $497\mu\text{s}$ a plot of equation 4.3 is shown in Figure 4.9.

The use of a fission chamber or cadmium-covered ^3He detector would result in unreasonable reactor operation time requirements. At the most subcritical condition, approximately three hours would be required to obtain data which would be statistically significant. In order to limit data collection times to a realistic value, all detector schemes except the cluster of four 15cm BF_3 detectors and the unshielded ^3He detector were eliminated.

Plots of count rate for various applied voltages for these detectors are shown in Figure 4.10. The rapid change in detector sensitivity at 1600V for the ^3He detector was unexpected and did not agree with the plateau data furnished with the detector. The plateau data for the cluster of four 15cm BF_3 detectors exhibited a more predictable result and therefore this detector scheme, operating at 2030V, was used in the final experiment.

The procedure used for the final experiment was as follows:

1. The startup source was inserted, and the control rods were moved to the desired reactor configuration.

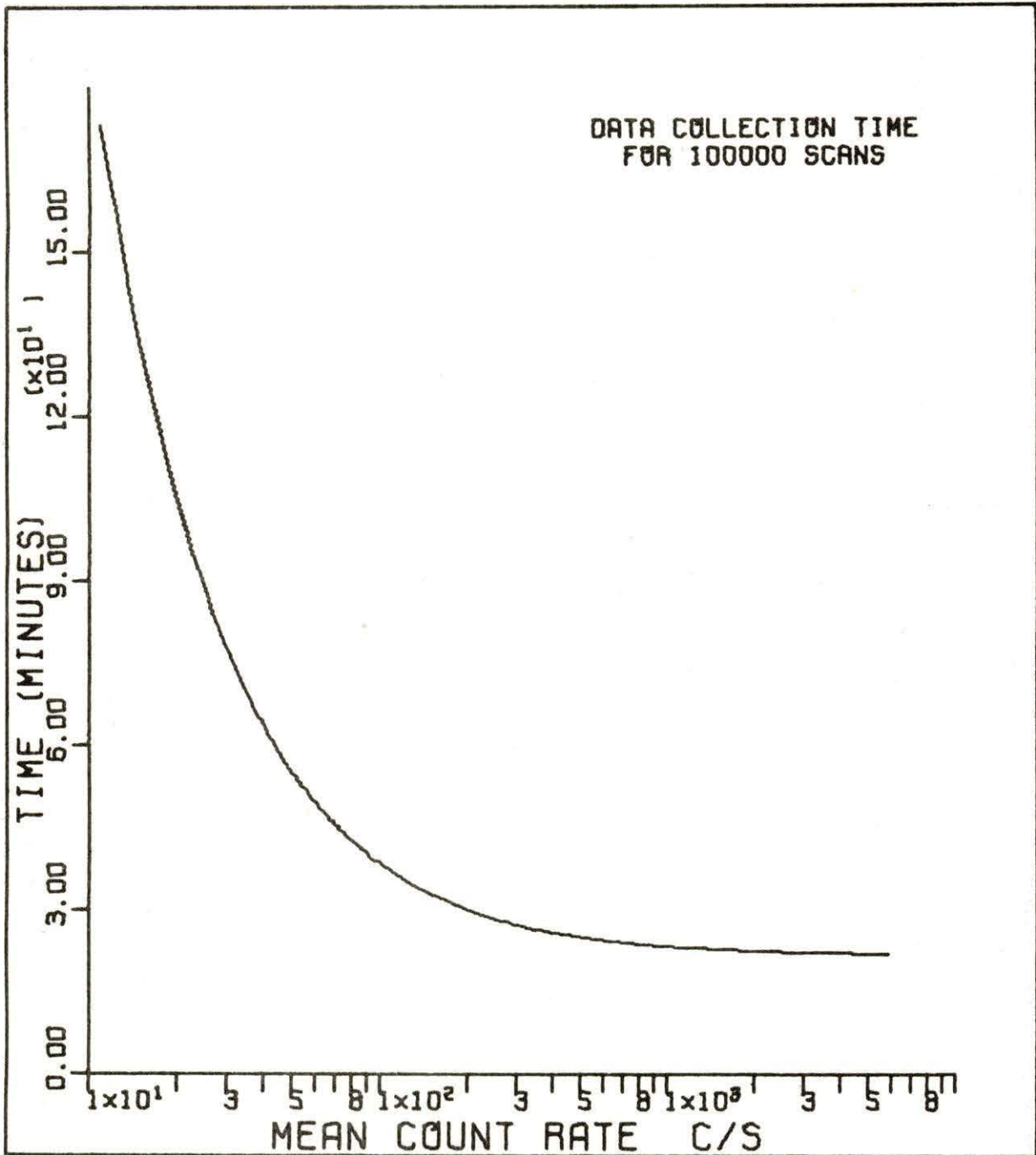


Figure 4.9. Influence of the average count rate on data collection times

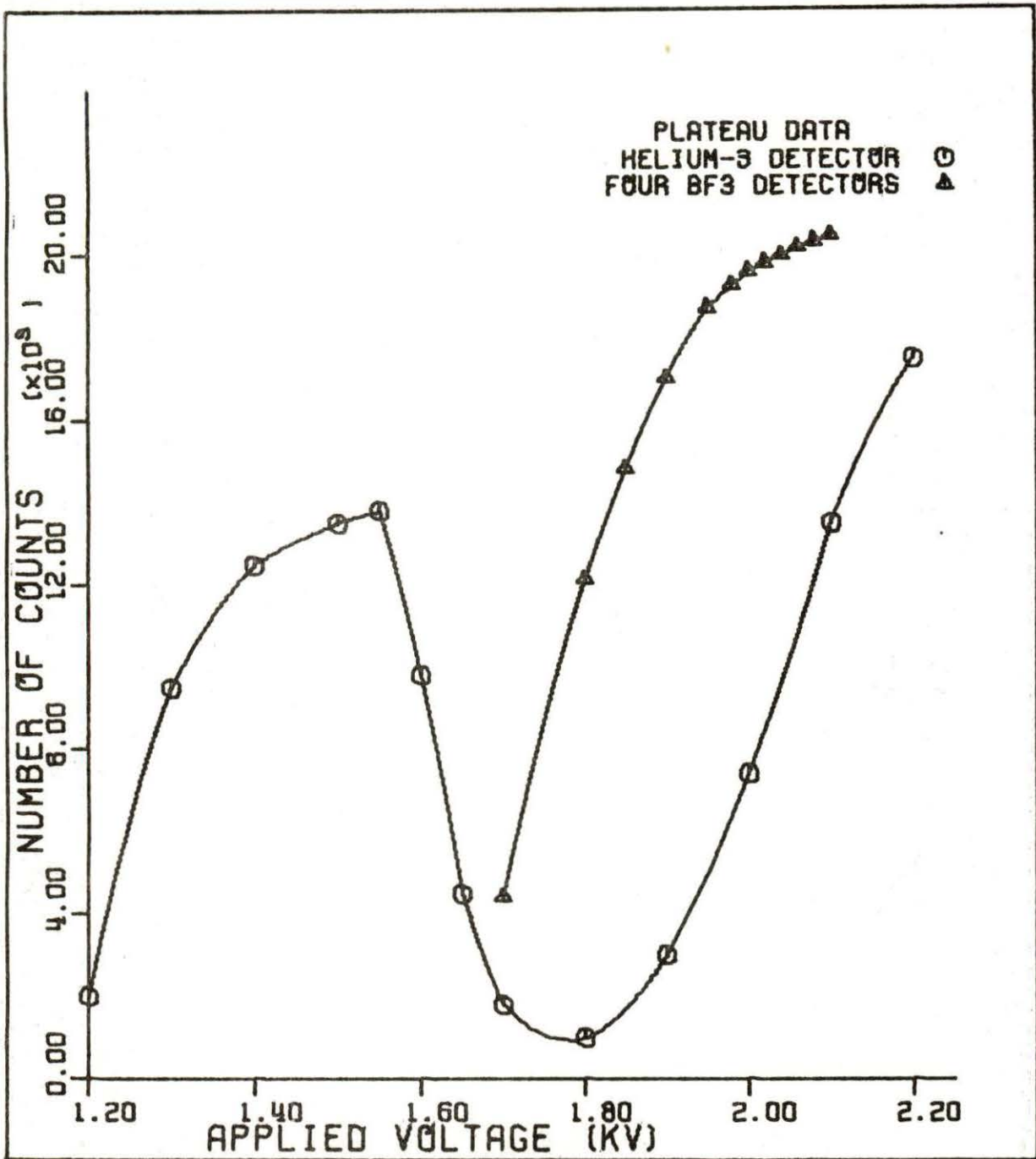


Figure 4.10. Effect of high voltage on count rate for ³He and BF₃ detectors

2. The startup source was removed and ten minutes were allowed to pass for the delayed neutron emission rate to reach equilibrium.
3. Prompt neutron decay data were collected based on 100,000 triggered scans. During this time an external scaler was used to obtain a highly accurate value for the average count rate.
4. After the data were output to the teletype, the startup source was inserted and a new reactor configuration was attained.

The reason for having the startup source out of the core during data collection was to achieve as low a power level as possible, thereby minimizing the value of n_p in equation 3.18. It was necessary to insert the source before changing reactor configuration in order to overcome a minimum count rate restriction interlocked to the control rod drive motors.

C. Analysis of Results

A typical plot showing the decay of neutron population following an initial neutron detection is presented in Figure 4.11. All of the control rods were fully inserted when this measurement was made. Based on a least-squares analysis, the prompt neutron decay constant was found to be 174 ± 7 radians/second. Decay plots for other reactor configurations are in Appendix B. The prompt neutron decay constants for

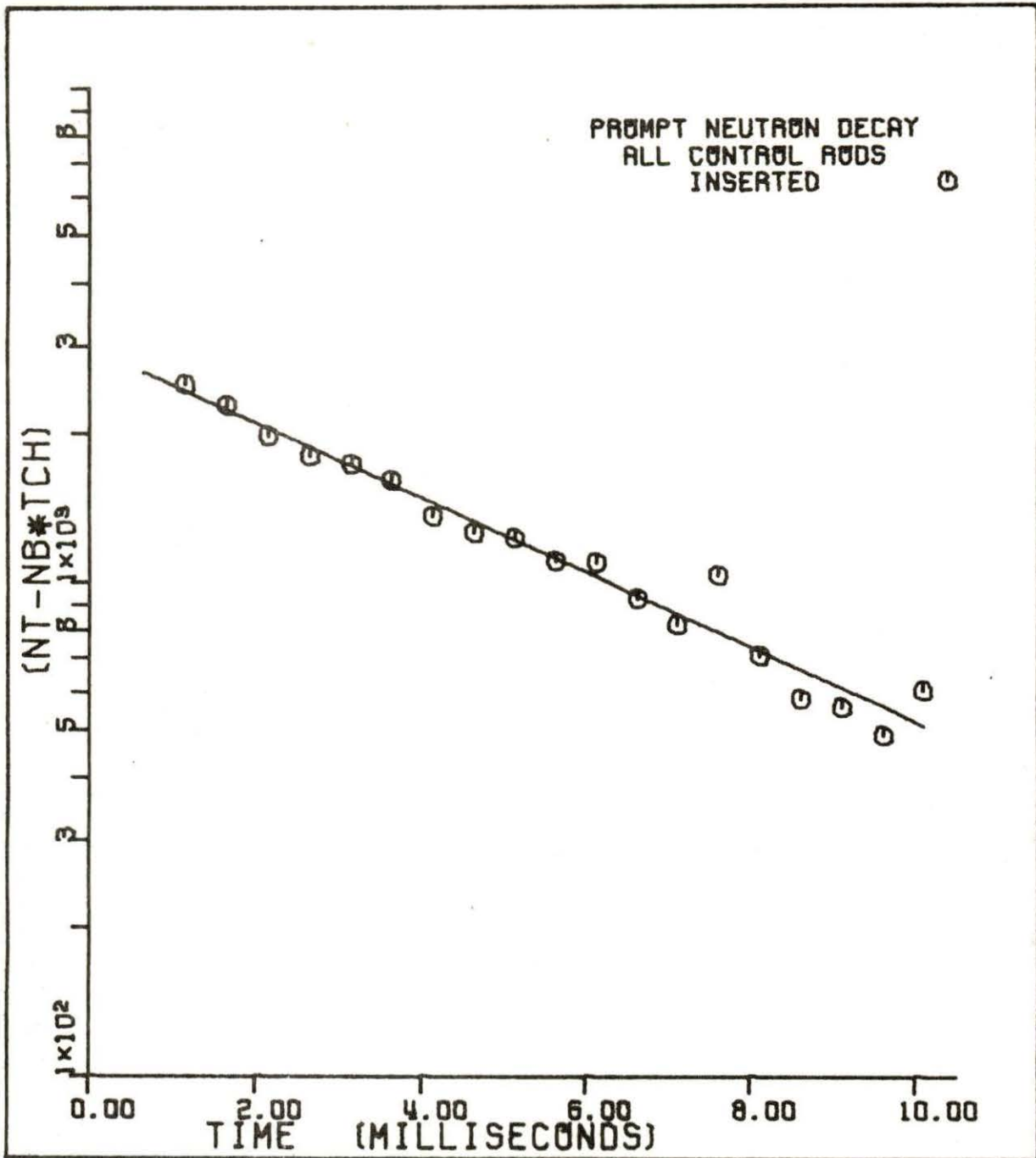


Figure 4.11. Decay of prompt neutrons with all control rods inserted

$$\alpha = 174 \text{ rad./s}$$

various reactor configurations are plotted against inverse mean count rate in Figure 4.12. Based on a least-squares analysis, the value of β/l was found to be 70 ± 7 radians/second. Table 4.1 summarizes the results obtained for this experiment based on $\alpha_0 = 70$ radians/second.

The errors assigned to the values in Table 4.1 are due to uncertainties in the measurement of the uncorrelated term and the statistical uncertainty based on the number of periods of exponential decay which were included in the data scan. Cohn [9] presents a method for determining the statistical uncertainty in an exponential decay measurement. Using Cohen's method of analysis for the decay constants in this experiment, the uncertainty resulting from using twenty channels is equivalent to the uncertainty that would result if an infinite number of channels were to have been used. This amounts to approximately 1 percent of the value of α . The uncertainty due to $t_{ch} N_{ch} = 10_{ms}$ ranges from a low of 1.7 percent at $\alpha = 174$ rad./s to a high of 5.3 percent at $\alpha = 94$ rad./s. An uncertainty of approximately 2 percent of results from the precision of the uncorrelated background measurement.

The reported prompt neutron decay constants were calculated without applying any corrections for the non-uniform channel widths shown in Figure 4.5.

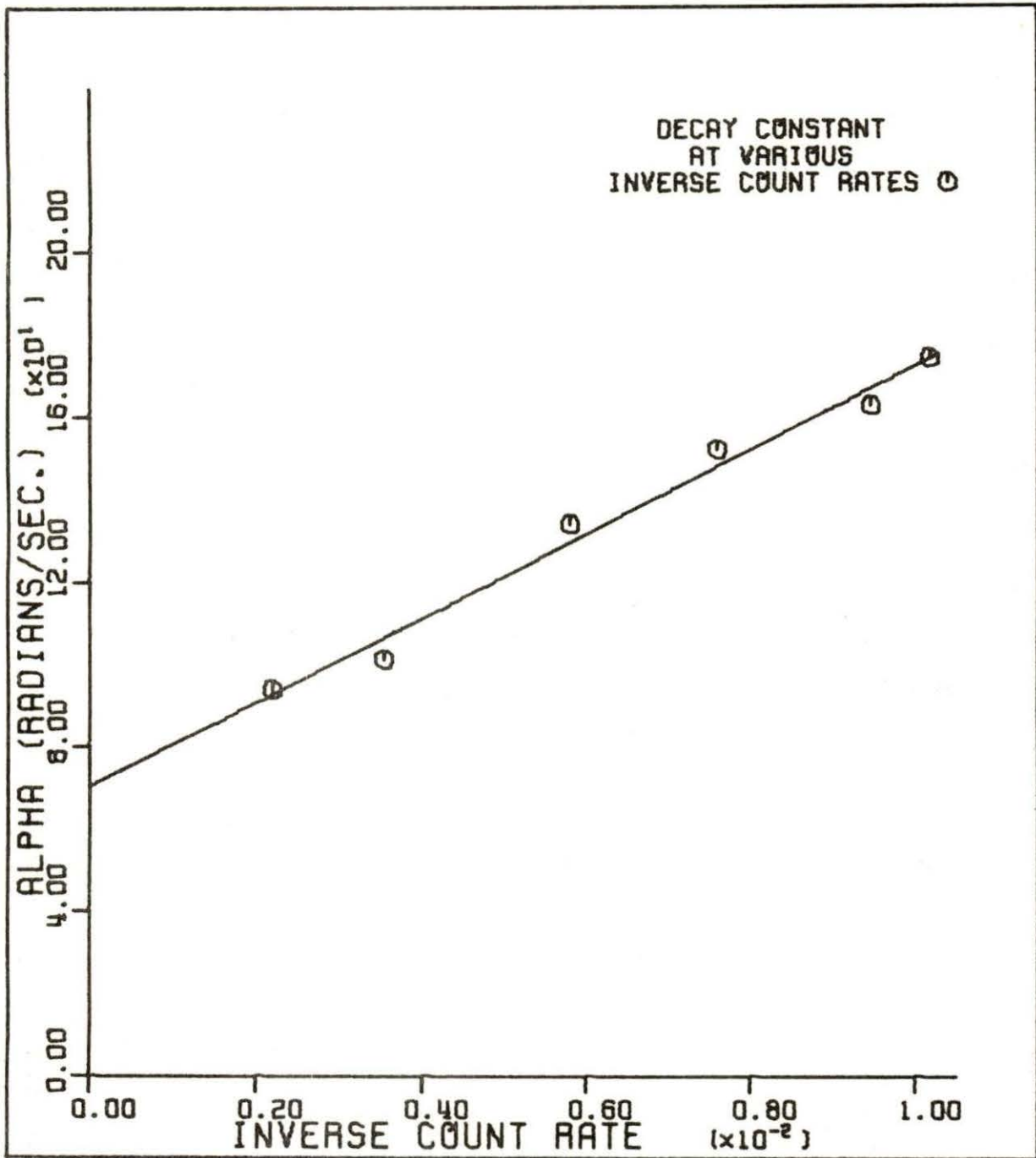


Figure 4.12. Prompt neutron decay constant for various reactor configurations

$$\alpha_0 = 70 \text{ rad./s}$$

The decay constants obtained from a calculation which included the nonuniform channel widths were well within the limits of uncertainty assigned to the initial results.

The $14\mu\text{s}$ to $20\mu\text{s}$ dead time between the detection of a trigger neutron and the initiation of the channel scan sequence was included as an average $17\mu\text{s}$ offset in the least-squares fitting routine. Neglecting this dead time would result in an additional error of 1 percent.

The results of prompt neutron decay measurements and subcriticality calculations based on these measurements are shown in Table 4.1. Control rod reactivity worths based on these measurements are compared to the values obtained from inverse kinetics measurements [13] in Table 4.2. The consistently low values of control rod worth for $\alpha_0 = 70 \text{ rad./s}$ indicate the presence of a systematic error or possibly an invalid assumption. The only parameter which could alter the value of all of the decay constants is the channel width. Since channel width calibrations were made several times and good agreement was obtained for each measurement this possibility was ruled out.

Based on frequency response and reactor noise measurements, Chan [8] and Nabavian [15] found the Rossi Alpha for the UTR-10 reactor to be approximately 45 rad./s . A theoretical calculation by Nodean [16] also supports this value. The relatively good agreement between inverse kinetics and prompt neutron decay measurements for safety 2, using $\alpha_0 = 45 \text{ rad./s}$,

Table 4.1. Experimental results, degree of reactor subcriticality

Reactor Configuration	α , rad./s	Dollars of Reactivity		Inverse Kinetics
		Prompt Neutron $\alpha_0=70$ rad./s	Decay Measurements $\alpha_0=45$ rad./s	
All control rods inserted	174 \pm 7	1.49	2.87	2.55
Safety 1 at 50% Safety 2 inserted	163 \pm 7	1.33	2.62	
Safety 1 withdrawn Safety 2 inserted	152 \pm 7	1.17	2.38	1.90
Safety 1 withdrawn Safety 2 at 30%	134 \pm 7	0.91	1.98	
Safety 1 withdrawn Safety 2 at 60%	101 \pm 7	0.44	1.24	
Safety 1 withdrawn Safety 2 withdrawn	94 \pm 7	0.34	1.08	0.60

Table 4.2. Control rod reactivity worths

Control Rod	Reactivity in Dollars		Inverse Kinetics
	Prompt Neutron $\alpha_0 = 70 \text{ rad./s}$	Decay Measurements $\alpha_0 = 45 \text{ rad./s}$	
Safety 1	0.32	0.49	0.70
Safety 2	0.76	1.30	1.25

indicates that equation 3.14 may not be valid for this situation. The discrepancy between the two methods in determining the reactivity worth of safety 1 is understandable in view of the large distance between the detector and safety 1 (approximately 130cm). This is consistent with Nabavian's [15] conclusion that subcriticality measurements are dependent upon detector location. By positioning the detector in the thermal column, measurements of reactivity changes in the north core are severely restricted due to the weak coupling between the two cores. Based on this observation one would expect that prompt neutron decay measurements would show the core to be further subcritical than is actually the case. Inspection of Table 4.1 confirms this expectation. The degrees of subcriticality in Table 4.1 were based on a normal reactor configuration with graphite stringers inserted. The removal of the graphite stringers was found to result in a negative reactivity insertion of 0.15 ± 0.02 dollars. Since the prompt neutron decay measurements were made with both stringers removed from the thermal column, the degrees of subcriticality listed in Table 4.1, based on inverse kinetics measurements, were corrected for this negative reactivity insertion. It was assumed that the effects from locating four BF_3 detectors in the thermal column could be neglected in comparison to the removal of the graphite stringers.

The absence of a second exponential characterizing an unreflected core is attributed to the relatively large channel widths employed and the presence of approximately 11cm of graphite between the detector and the fuel. Locating the detector within a fuel assembly would increase the probability of detecting neutrons which have not experienced collisions in the reflector between fission events. Resolving this exponential would require channel widths of less than $100\mu\text{s}$ which is beyond the capability of the present data acquisition system. Using shorter channel widths would also increase the data collection time considerably. Modifications which could be made to the existing hardware and software in order to obtain shorter channel widths are discussed in Appendix C.

V. CONCLUSIONS

The use of a microcomputer-based data acquisition system resulted in a substantially superior data collection system in comparison to the available multichannel analyzers. Channel width deviation was within 1 percent of the mean channel width, and the flexibility in choosing the channel width and number of channels to be scanned allowed the data collection time to be minimized. Since only software modifications were required to make these changes the hardware configuration of the system was independent of these parameters.

The dead time between channels was less than $1\mu\text{s}$ due to the use of two counters on the counter-timer peripheral. It was therefore unnecessary to apply correction factors for interchannel dead times.

The dead time between the detection of a trigger neutron and initiation of the channel scan sequence ranged from $14\mu\text{s}$ to $20\mu\text{s}$. This dead time was not a serious limitation since the experiment was not acutely sensitive on the exact timing of the channel scan. Compensation for this dead time was easily included in the data fitting process.

Development of a microcomputer-based data acquisition system with sufficient memory to allow data analysis (approximately 16K) costs approximately \$1100. A multichannel analyzer with similar specifications costs approximately

\$5000. The microcomputer system, however, is readily interfaced to other experiments requiring data acquisition and analysis. The multichannel analyzer is limited to the traditional energy spectrum, event counting experiments with little or no calculating ability.

Application of the point kinetics equations for prompt neutron decay measurements on the UTR-10 coupled-core reactor yielded unsatisfactory results when the detector was located a substantial distance from the disturbance. The point reactor model seemed to be valid if measurements were constrained to a single core and if the detector was located close to that core.

All of the decay constants observed were characteristic of a reflected core. The unreflected prompt neutron decay constants were not observed primarily due to an 11cm graphite reflector located between the detector and the south core. The value of the Rossi Alpha was found by extrapolation to be 70 ± 7 rad./s which disagrees with the value of 45 rad./s found by Nabavian [15] and Chan [8]. This discrepancy was attributed to the limitations of the point reactor model based on the location of the detector.

Neutrons which are correlated in time to fission events do not necessarily have energies greater than 0.4eV. Shielding a detector with a thermal neutron absorber is therefore not an acceptable means of increasing the detector figure of merit.

Low detector sensitivities result in higher figures of merit and therefore, yield data which are less sensitive to the uncorrelated component. Unfortunately these higher figures of merit are associated with low count rates, and usually must be compromised in order to obtain reasonable data collection times.

VI. REFERENCES

1. Albrecht, R. W. 1961. The Measurement of Dynamic Nuclear Reactor Parameters by Methods of Stochastic Processes. Trans. Am. Nuc. Soc. 4(2):311-312.
2. Auerbach, J. M., and S. G. Carpenter. 1978. A Microprocessor Controlled Reactivity Meter for Real Time Monitoring of Reactors. IEEE Transactions on Nuclear Science 25(1):98-100.
3. Babala, D. 1966. Technical Notes: On the Theory of the Rossi Alpha Experiment in Reactor Noise Studies. Nucl. Sci. Eng. 26:418-424.
4. Bierman, R. R., K. L. Garlid, and R. W. Albrecht. 1965. Complementary Use of Pulsed-Neutron and Reactor-Noise Measurements. Nucl. Sci. Eng. 22:206-214.
5. Brunson, G. S., R. Curran, S. G. Kaufmann, J. McMahon, and L. Pahis. 1957. Measuring the Prompt Period of a Reactor. Nucleonics 15(11):132-141.
6. Brunson, G. S., R. L. McVean, P. I. Anderson, and J. M. Gasidlo. 1963. Critical Studies of a Small Uranium Carbide-Fueled Reactor with a Beryllium Reflector. U. S. Atomic Energy Commission Report ANL-6713. (Argonne National Laboratory, Lemont, Ill.) 19 pp.
7. Bryce, Donald H. 1964. Measurement of Reactivity and Power Through Neutron-Detection Probabilities. Pages 61-76 in Robert E. Uhrig, ed. Noise Analysis in Nuclear Systems. U. S. Atomic Energy Commission, Washington, D. C. TID-7679.
8. Chan, Te-Chang. 1971. Reactor Transfer Function Measurements with the Reactor Oscillator. M. S. Thesis. Iowa State University, Ames, Iowa. 82 pp.
9. Cohn, C. E. 1965. On the Precision of Measurements of Exponential Growth and Decay Constants. U. S. Atomic Energy Commission Report ANL-7110. (Argonne National Laboratory, Lemont, Ill.)
10. De Clercq, A., E. Jacobs, D. De Frenne, H. Thierens, P. D'Hondt, and A. J. Deruytter. 1977. A Versatile CAMAC-Based Linear PHA System. Nuclear Instruments and Methods 144:593-596.

11. Hetrick, David L. 1971. Dynamics of Nuclear Reactors. The University of Chicago Press, Chicago, Ill. 540 pp.
12. Kumahara, T., H. Yagi, S. Inomata, I. Ohuchi, and T. Takeda. 1978. A Micro-CAMAC System for Use in a Gamma Spectrometry System. IEEE Transactions on Nuclear Science 25(1):485-488.
13. Meyer, Douglas J. 1976. UTR-10 Reactivity Control. Report for Nuclear Engineering 541. Iowa State University, Ames, Iowa.
14. Mos Technology. 1976. KIM-1 User Manual. Mos Technology, Norristown, Pa. 80 pp.
15. Nabavian, Massoud. 1973. Reactor Noise Measurements in the UTR-10 Using the Polarity Correlation Method. M. S. Thesis. Iowa State University, Ames, Iowa. 93 pp.
16. Nodean, Walter Charles. 1969. The Response of a Coupled Core Reactor to a Localized Oscillation of the Absorption Cross Section. Ph. D. Dissertation. Iowa State University, Ames, Iowa. 98 pp.
17. Orndoff, J. D. 1957. Prompt Neutron Periods of Metal Critical Assemblies. Nucl. Sci. Eng. 2:450-460.
18. Pacilio, Nicola. 1968. A survey of Reactor-Noise Time-Analysis Methods. Batelle Northwest Laboratory Report BNWL-875. Richland, Washington. 45 pp.
19. Pacilio, Nicola. 1969. Reactor Noise Analysis in the Time Domain. U. S. Atomic Energy Commission, Washington, D. C. TID-24512. 102 pp.
20. Silberberg, Jeffery L. 1977. A Microprocessor System for a Portable Neutron Spectrometer/Kerma-Rate Meter. IEEE Transactions on Nuclear Science 24(1):386-390.
21. Soucek, Branko. 1976. Microprocessors and Microcomputers. John Wiley and Sons, New York. 607 pp.
22. Thie, Joseph A. 1963. Reactor Noise. Rowman and Littlefield, Inc., New York. 262 pp.

VII. ACKNOWLEDGMENTS

The author wishes to express his gratitude to the Iowa State University Microcomputer Research Group for the temporary use of a KIM-1 microcomputer and their cooperation throughout this study.

Consultations during the development of the software for the data acquisition system with Dr. T. A. Smay were very illuminating and greatly appreciated.

The author would like to express a special appreciation to his major professor, Dr. Richard A. Hendrickson, for his advice and assistance during this study. His unfailing tolerance and good humor during some of the dark moments of equipment development were greatly appreciated.

It is also a pleasure to express appreciation to electronic technician Elden Plettner and reactor operators Soli Khericha and Lung-Rui (George) Huang for their cooperation and assistance.

VIII. APPENDIX A:

COUNTER-TIMER PERIPHERAL

A schematic of the counter-timer peripheral device is shown in Figure 8.1. Pulses leaving the pulse height discriminator have an amplitude of approximately 8 volts and a width of $2\mu s$. The output of the pulse height discriminator is converted to 5 volt logic by simply driving transistor Q1, a 2N3904, to saturation. The inverter following Q1 is used to return the pulse to a positive spike for counting purposes.

Counters 1 and 2 are binary coded decimal counters and are both contained within a single package (Motorola C4033P). The enable gates (E) of the counters were tied to +5 volts to prevent the counters from incrementing on the negative edge of the enable pulse. Enabling of the individual counters was accomplished through the use of dual input NAND gates followed by inverters.

The timer circuit consists of a 1MHz oscillator followed by eight J-K flip-flops, each equipped with a clear function. The 1MHz clock oscillator operates continuously and in case of failure, provisions were made to allow an external clock to be implemented through a BNC connector located on the printed circuit board. The \overline{IRQ} line to the KIM-1 microcomputer is held high when the flip-flops are in the clear state (port B, bit 5 = 0). When the timer is started (port B, bit 5 = 1), the cascade of flip-flops divides the clock output

by 2^8 . For the 1MHz clock output used, the $\overline{\text{IRQ}}$ is driven low $128\mu\text{s}$ after the timer is started. This line stays low for an additional $128\mu\text{s}$ which is ample time for the micro-computer to service the interrupt and reset the clock. Since the flip-flops are edge triggered, the maximum delay between receiving a start signal and the initiation of the divide-by sequence is one cycle or $1.0\mu\text{s}$ for a 1MHz clock (square wave).

Definitions of the individual peripheral data bits are provided in Table 8.1. Table 8.2 shows the result of storing various hexadecimal values into port B data when port B bits zero through five are configured as outputs. The values listed include all of the values used in programs ROSSI.SRC and VARMEN.SRC.

The hardware cost for development and construction of the counter-timer peripheral, including power supply, was approximately \$150. The amount of time required for hardware development was estimated at 20 hours.

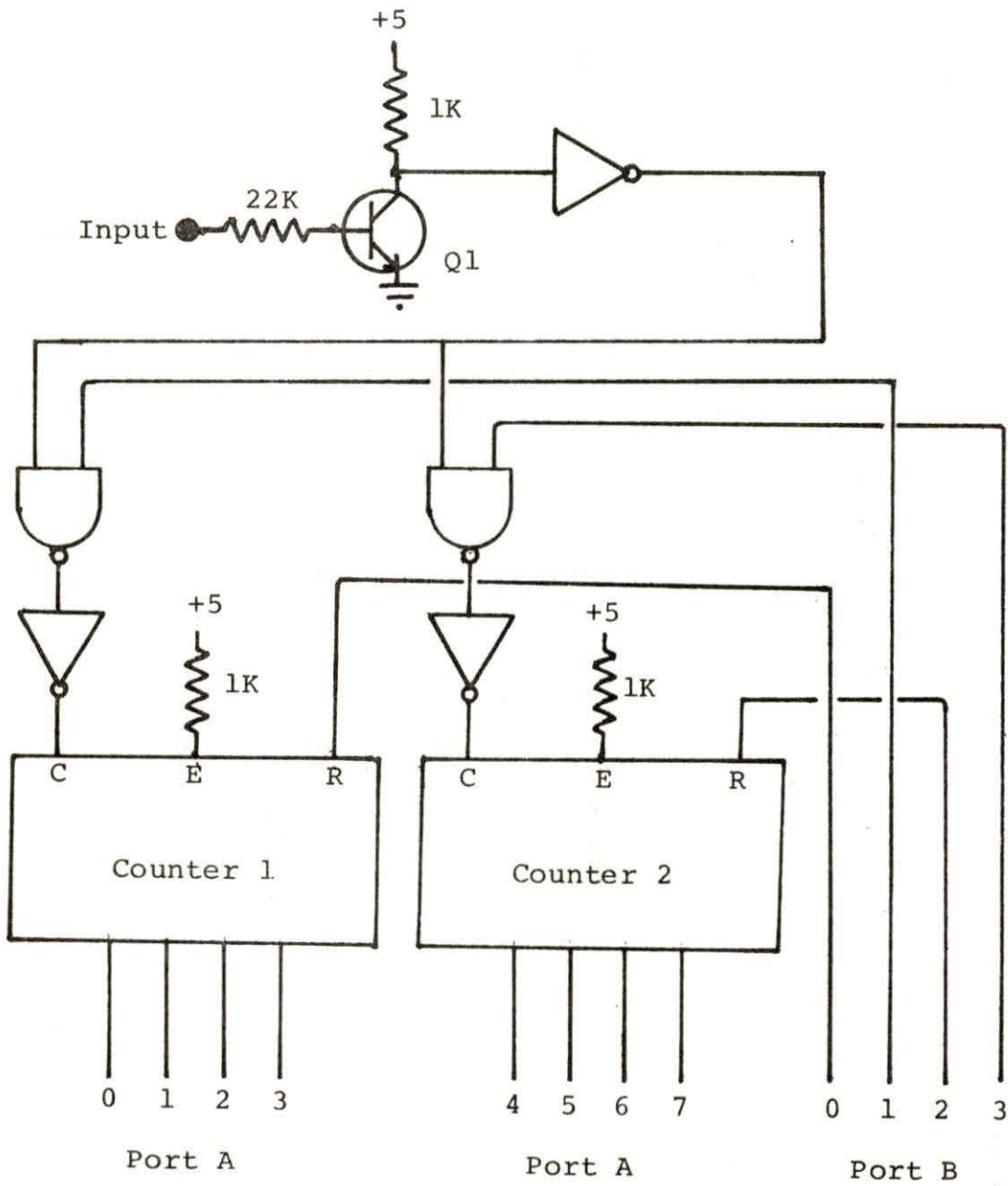


Figure 8.1. Counter-timer peripheral

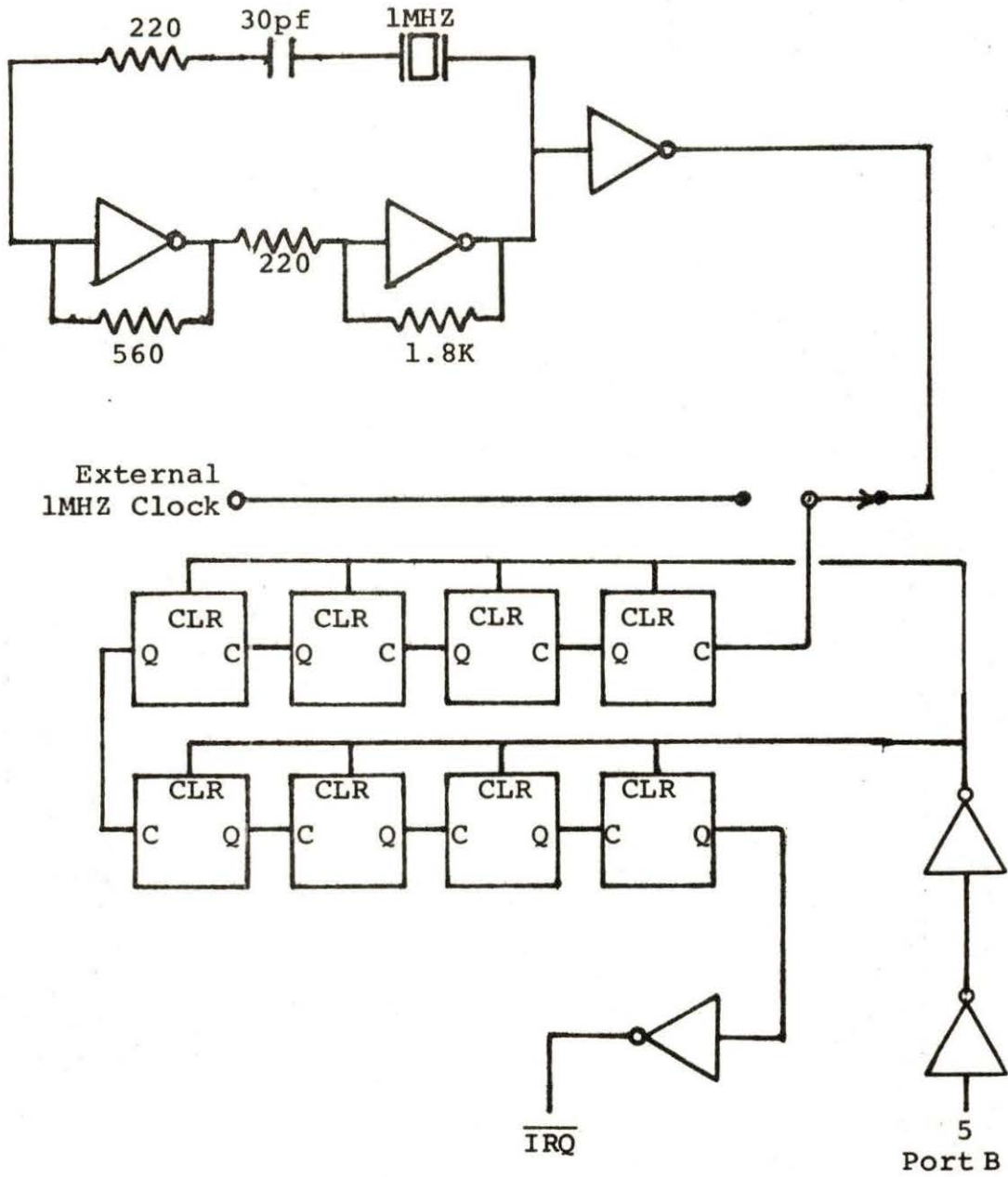


Figure 8.1 continued

Table 8.1. PIA 6530-003 data bit definitions

Port	Data Bit	Function
B	0	Reset counter 1 when high
B	1	Enable counter 1 when high
B	2	Reset counter 2 when high
B	3	Enable counter 2 when high
B	4	Not used
B	5	Enable timer when high, reset timer when low
B	6	Not used
B	7	Not used
A	0	Counter 1 data
A	1	
A	2	
A	3	
A	4	Counter 2 data
A	5	
A	6	
A	7	

Table 8.2. Useful hexadecimal values for control of counter-timer peripheral

Hexidecimal Value Stored at Port B Data	Timer	Counter 1	Counter 2
00	Reset	Disable	Disable
02	Reset	Enable	Disable
05	Reset	Reset	Reset
06	Reset	Enable	Reset
08	Reset	Disable	Enable
09	Reset	Reset	Enable
22	Enable	Enable	Disable
26	Enable	Enable	Reset
28	Enable	Disable	Enable
29	Enable	Reset	Enable

IX. APPENDIX B:
PROMPT NEUTRON DECAY PLOTS

Graphs depicting the decay of prompt neutrons following a fission event are shown in Figures 9.1 through 9.5 for various reactor configurations. These data were obtained using the KIM-1 microcomputer-based data acquisition system with routine ROSSI.SRC. A total of 100,000 triggered scans of twenty channels were used for each plot. The channel width was $497 \pm 5 \mu\text{s}$. Due to the large channel width error in channel 1 this datum point was not used in the least-squares fitting and is therefore not shown in the accompanying figures.

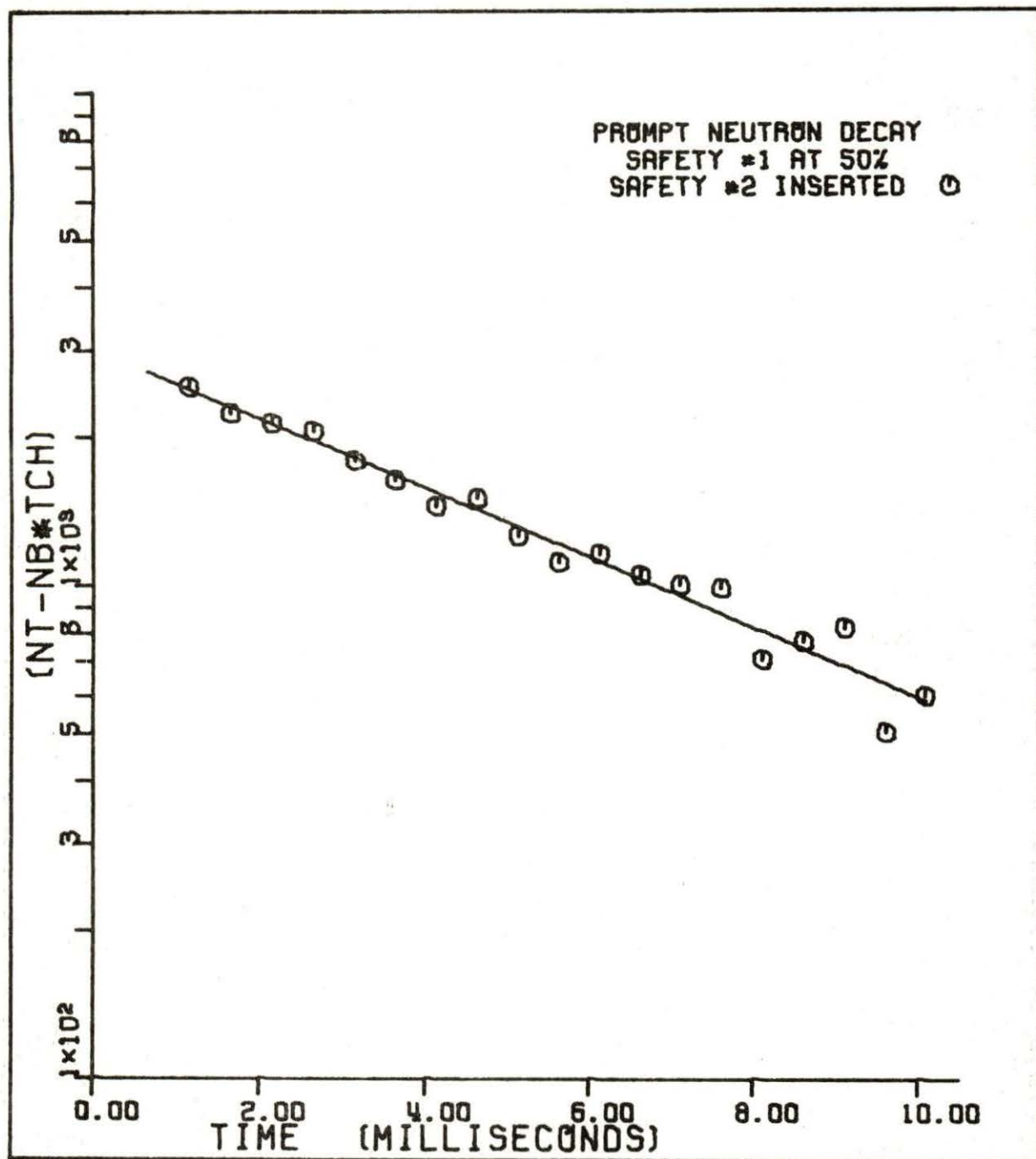


Figure 9.1. Prompt neutron decay with safety 1 50 percent withdrawn and safety 2 fully inserted

$$\alpha = 163 \pm 7 \text{ rad./s}$$

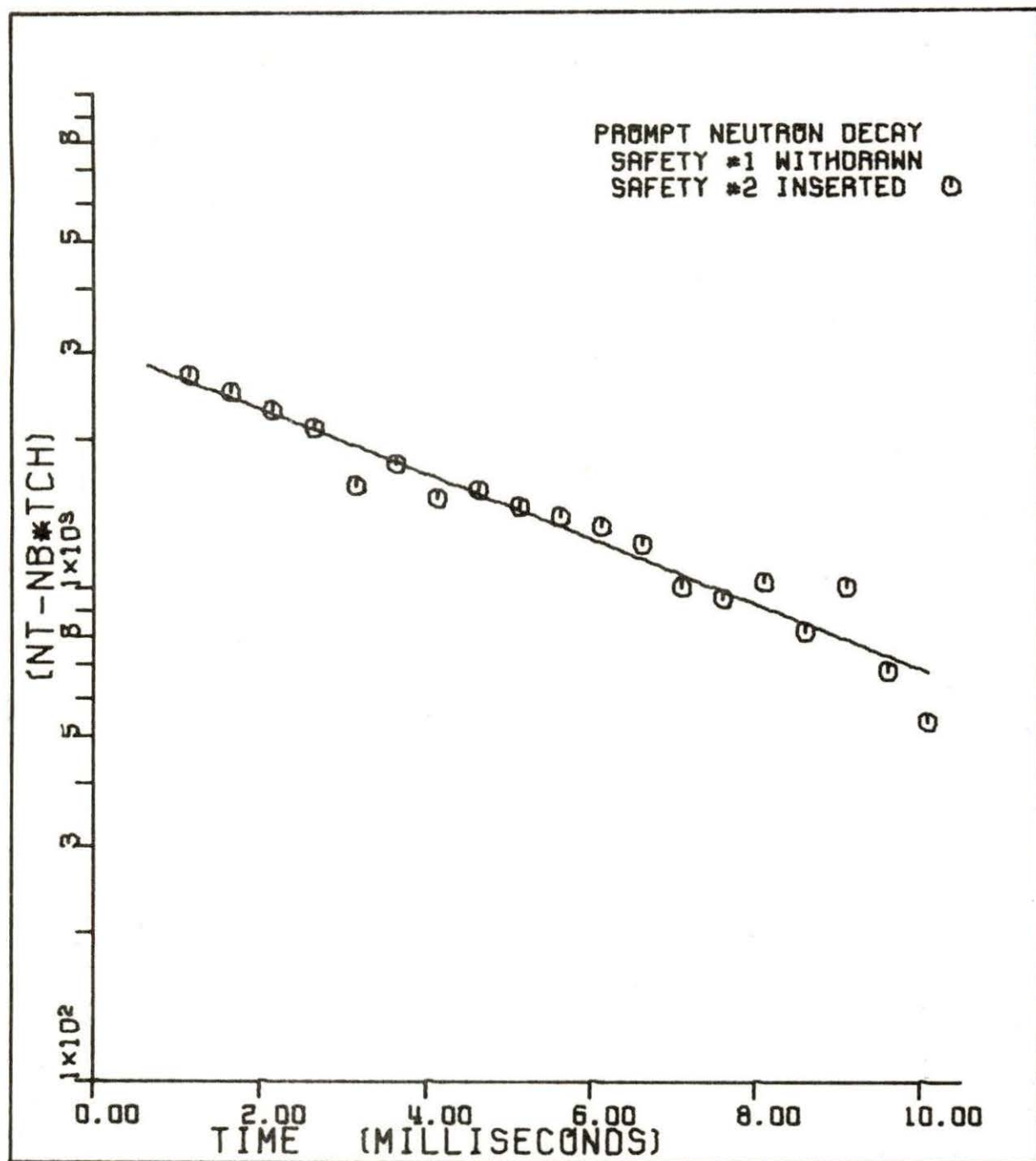


Figure 9.2. Prompt neutron decay with safety 1 fully withdrawn and safety 2 fully inserted

$$\alpha = 152 \pm 7 \text{ rad./s}$$

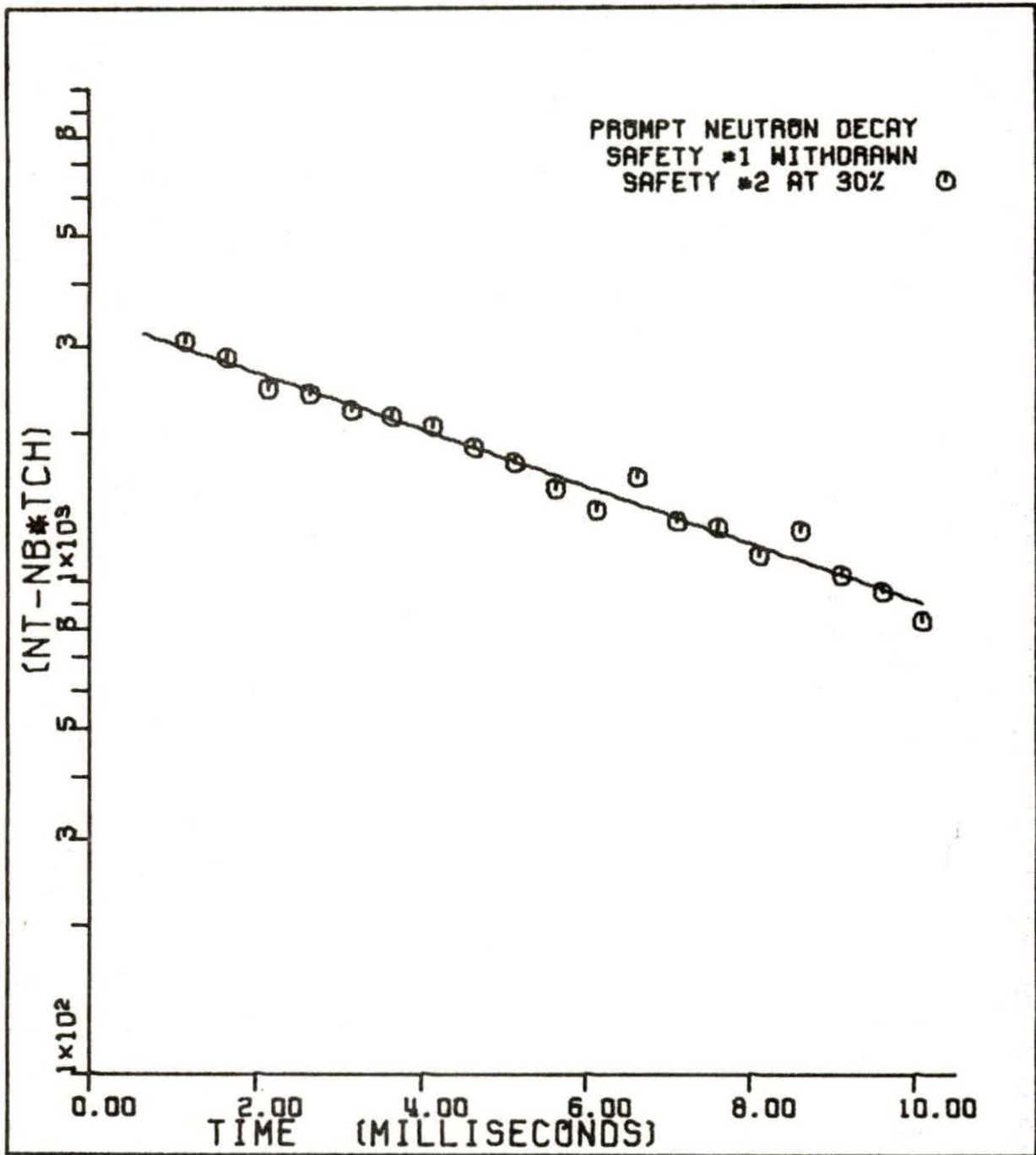


Figure 9.3. Prompt neutron decay with safety 1 fully withdrawn and safety 2 30 percent withdrawn

$$\alpha = 134 \pm 7 \text{ rad./s}$$

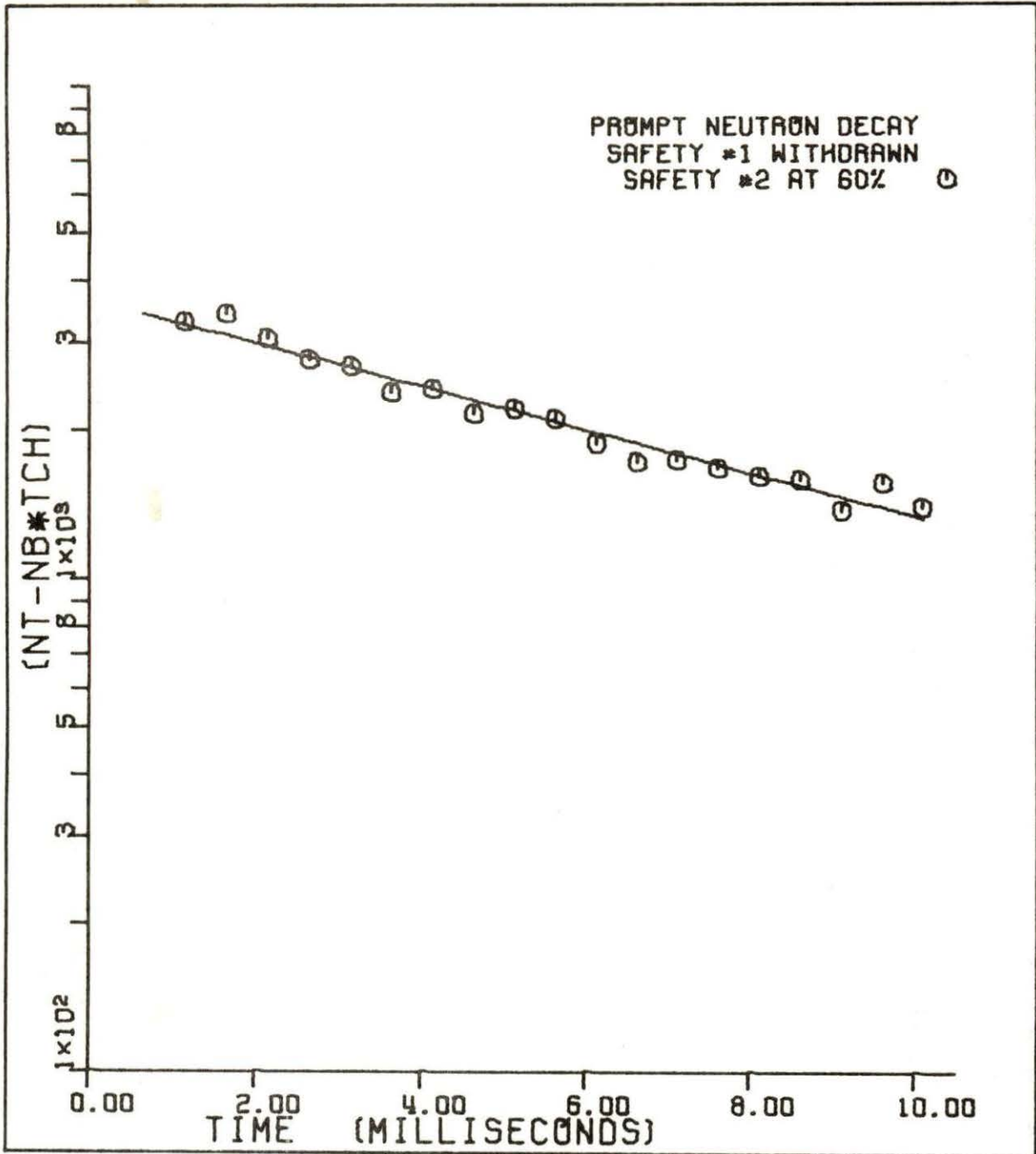


Figure 9.4. Prompt neutron decay with safety 1 fully withdrawn and safety 2 60 percent withdrawn

$$\alpha = 101 \pm 7 \text{ rad./s}$$

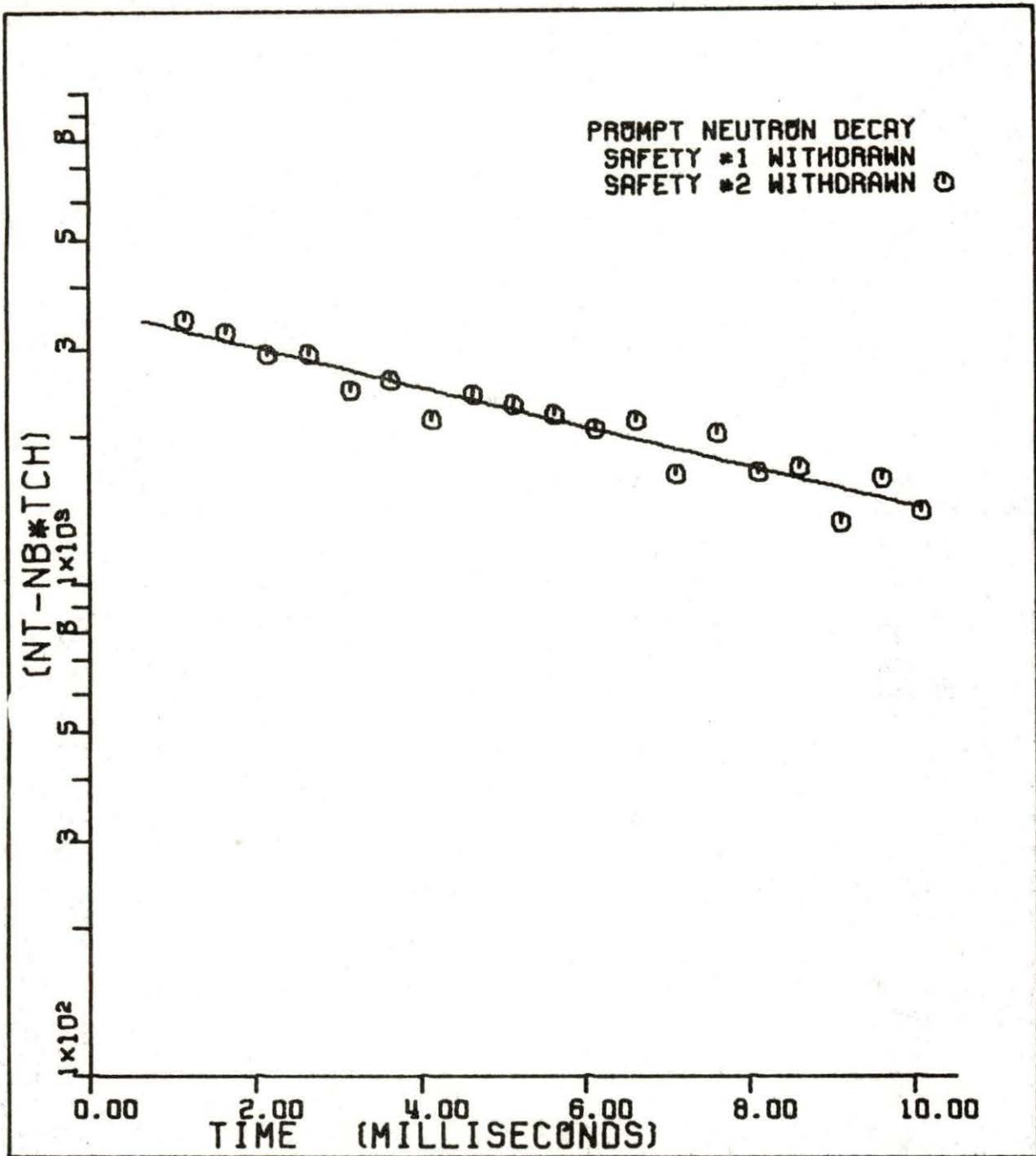


Figure 9.5. Prompt neutron decay with safety 1 fully withdrawn and safety 2 fully withdrawn

$$\alpha = 94 \pm 7 \text{ rad./s}$$

X. APPENDIX C:

DATA COLLECTION ROUTINE ROSSI.SRC

A. Description of ROSSI.SRC

A listing of routine ROSSI.SRC is located in section B of this appendix. Execution of ROSSI.SRC starting at ZROMEM clears the area of memory used for storing the counts accumulated in each channel. Execution then continues into routine SYSINT which initializes the peripheral interface adapter (6530-003) for data transfers between the micro-computer and the counter-timer peripheral. The accumulation of additional data after program execution has been terminated is accomplished by restarting the program at routine SYSINT.

Recognition of the trigger neutron, which starts the channel scan sequence, occurs in the loop labeled WAIT. The contents of counter 1 are compared to the accumulator which is zero. When counter 1 exceeds zero the program falls through the loop and the channel scan sequence begins. If the trigger neutron is detected immediately preceding the execution of the compare instruction, a dead time of $14\mu\text{s}$ will result before initiation of the channel scan as a result of resetting counter 1 and starting the timer. If the trigger neutron is detected immediately after execution of the compare instruction, loop WAIT is passed through one additional time which adds $6\mu\text{s}$ to this dead time. Using this algorithm for trigger detection will always result in a dead time which may vary as

much as $\pm 3\mu\text{s}$. The overall dead time could be reduced $6\mu\text{s}$ by enabling counter 2 instead of counter 1 in loop WAIT. This would eliminate the need to reset counter 1 before starting the channel scan.

During the time a channel is open (counter 1 or 2 enabled) data from the previous count are stored. A call to subroutine DATADD results in the data being summed with counts which were present from previous scans (in a given channel). Since both counters share the same data port, it is necessary to shift the data to eliminate any counts which may have accumulated in the active counter prior to reading the data port. This shifting must also insure that the new data being added is located in the four least significant bits of the data byte.

The algorithm used for determining channel width is based on an external timer on the counter-timer peripheral. The timer is started coincidentally with the enabling of a channel. After the data from the previous counter are stored, the interrupt request is enabled, and the program loops (TST1, TST2, or TST3) until the timer signals an interrupt request after $128\mu\text{s}$. Upon entering the IRQ service routine a loop is encountered which may be used to increase the channel width. By increasing the value at \$02FA (corresponding to the LDY instruction), the channel width may be increased $7\mu\text{s}$ per loop execution. After leaving

this loop the timer is reset and the main program execution continues. The presently enabled counter is disabled in coincidence with the enabling of the other counter and starting of the timer. Deviation in channel width results from the occurrence of the interrupt with respect to the instruction currently being executed. The loop must be passed through an additional time if the interrupt occurs immediately after the compare instruction was executed. This results in a predicted channel width deviation of $\pm 5 \mu\text{s}$.

The channel width deviation and range of dead times preceding the initiation of the channel scan are due to basically the same mechanism. The channel width deviation could be reduced by use of a different microprocessor, the M6800. The instruction set for this processor includes a wait for interrupt instruction [12] which allows the processor to respond to an interrupt within one machine cycle of its occurrence. If the trigger algorithm was also based on an interrupt request (which would require additional hardware) the range of dead times could also be reduced to plus or minus one machine cycle. One version of the 6800 μP is capable of operating with a 2MHz clock. The channel width deviation and dead time range would be expected to be on the order of $\pm 0.5 \mu\text{s}$ using this processor.

The use of a 2MHZ microprocessor would also allow shorter channel widths. The 128 μ s timer was chosen based on the maximum time required to accomplish data handling for the previous channel. Since the KIM-1 uses a 1MHZ clock, conceivably the minimum channel width could be reduced to less than 100 μ s if a 2MHZ microprocessor was used.

The teletype output routine, TTYOUT, is executed automatically after 100,000 channel scans, or may be manually invoked by the nonmaskable interrupt. Data collection is discontinued and the counts accumulated in the channels are output to the teletype, each channel on a different line. Extensive use is made of the output routines located in the read-only memory [14]. The last value output is the number of channel scans.

Following the data output routine BKGND collects uncorrelated counts for a total time equal to that of each individual channel in the triggered sequence. This background value is then output to the teletype along with the number of scans completed. The number of background scans is equal to the number of triggered scans. At the conclusion of this routine the program goes into an infinite loop. Control is returned to the monitor program by resetting the microcomputer.

Approximately 80 hours was required for software development. This relatively large amount of time is a result of changes made to the counter-timer peripheral during software development.

B. Source Code Listing of ROSSI.SRC

```

;ROSSI.SRC
;THIS ROUTINE ACQUIRES NEUTRON COUNTS CORRELATED TO FISSION CHAINS
;BY ACCUMULATING COUNTS IN TWENTY SEQUENTIAL CHANNELS.
;THE CHANNEL SCAN SEQUENCE IS INITIATED BY A RANDOM NEUTRON DETECTION.
;CHANNEL WIDTH IS DETERMINED BY THE VALUE STORED AT LOCATION $02FA.
;THE DEFAULT VALUE IS 176 MICROSECONDS.
;AN AVERAGE OF 17 MICROSECONDS ELAPSES BETWEEN THE DETECTION OF A
;TRIGGER NEUTRON AND THE INITIATION OF THE CHANNEL SCAN SEQUENCE.
;CHANNEL DEAD TIMES ARE ESTIMATED TO BE WELL BELOW 1 MICROSECOND
;DATA IS OUTPUT TO THE TELETYPE AFTER 100000 SCANS
;OR IN RESPONSE TO THE NONMASKABLE INTERRUPT.

```

```

;
;*****

```

```

; **

```

```

; **          CHANNEL WIDTH DATA

```

```

; **

```

```

; **

```

```

; **

```

```

; **

```

```

; **

```

```

; **

```

```

; **

```

```

; **

```

```

; **

```

```

; **

```

```

; **

```

```

; **

```

```

; **

```

```

; **

```

```

; **

```

```

; **

```

```

; **

```

```

; **

```

```

; **

```

```

; **

```

```

; **

```

```

; **

```

```

; **

```

```

; **

```

```

; **

```

```

; **

```

```

; **

```

```

; **

```

```

; **

```

```

CHANNEL WIDTH
(MICROSECONDS)

```

```

176
233
296
360
425
497
560
615
680
805
925
1060
2200

```

```

HEXIDECIMAL VALUE
STORED AT MEMORY
LOCATION $02FA

```

```

01
08
10
18
20
29
30
38
40
50
60
70
FF

```

```

;*****

```

```

;

```

```

PRTBYT=$1E38
CRLF=$1E2F
INIT1=$1E8C
TMPX=$05
TMPY=$06
CT=$07
DATA=$0340
PADD=$1701
PBDD=$1703
PAD=$1700
PBD=$1702
IRQL=$17FE
IRQH=$17FF
NMIL=$17FA
NMIH=$17FB
SCANLL=$037C
SCANL=$037D
SCANH=$037E
BGLL=$03FD
BGL=$03FE
BGH=$03FF
BKGLL=$03FA
BKGL=$03FB
BKGH=$03FC
;
*=0200
;ZROMEM
;ZEROS MEMORY BETWEEN $0340 AND $037F
ZROMEM SEI
      CLC
      LDX #00
      TXA
ZERO  STA DATA,X
      INX
      CPX #$3F

```

```

BCC ZERO
;
;SYSINT
;SYSTEM INITIALIZATION ROUTINE
SYSINT SEI
LDX #$FF
TXS           ;INITIALIZE STACK POINTER
JSR INIT1
JSR CRLF     ;OUTPUT CR/LF TO CONFIRM PROGRAM EXECUTION
LDA #00
STA PADD     ;SET UP PORT A AS INPUTS
LDA #$3F
STA PBDD     ;SET UP LOWER 6 BITS OF PORT B AS OUTPUTS
LDA #$80
STA NMIL
LDA #$03
STA NMIH     ;SET NMI VECTOR AT $0380 FOR OUTPUT ROUTINE
LDA #00
STA PBD      ;DISABLE COUNTERS AND TIMER
LDA #$F9
STA IRQL
LDA #$02
STA IRQH     ;SET IRQ VECTOR AT $02F9 FOR TIMER ROUTINE
SYS1 LDA #$05
STA PBD      ;RESET BOTH COUNTERS
LDX #00      ;ZERO CHANNEL COUNTER AND MEMORY INDEX
LDA #$02
STA PBD      ;ENABLE COUNTER 1
LDA #$00
WAIT CMP PAD
BEQ WAIT     ;WAIT FOR TRIGGER PULSE
LDA #$05
STA PBD      ;RESET COUNTER(S)
LDA #$22
STA PBD      ;START COUNTER 1, START TIMER

```

```

CLC
SED ;INCREMENT SCAN COUNTER
LDA SCANLL
ADC #$01
STA SCANLL
BCC SCAN1
CLC
LDA SCANL
ADC #01
STA SCANL
BCC SCAN1
CLC
LDA SCANH
ADC #01
STA SCANH
SCAN1 CLC
CLD
LDA PBD
CLI
TST1 CMP #$22
BEQ TST1 ;WAIT FOR IRQ FROM TIMER
SEI
LDA #$28
STA PBD ;STOP COUNTER 1, START COUNTER 2, START TIMER
LDA PAD
RTN1 CLC ;SCAN FOR TEN ITERATIONS (20 CHANNELS)
ASL A ;SHIFT COUNTER 1 DATA TO ELIMINATE ANY COUNTS
ASL A ;WHICH MAY HAVE OCCURRED IN COUNTER 2
ASL A
ASL A
JSR DATADD ;ADD DATA FROM COUNTER 1 TO MEMORY
LDA #$29
STA PBD ;RESET COUNTER 1
CLI
TST2 CMP #$29

```

```

        BEQ TST2           ;WAIT FOR IRQ FROM TIMER
        SEI
        LDA #$22
        STA PBD           ;STOP COUNTER 2, START COUNTER 1, START TIMER
        LDA PAD
        JSR DATADD       ;ADD DATA FROM COUNTER 2 TO MEMORY
        LDA #$26
        STA PBD           ;RESET COUNTER 2
        CLI
TST3    CMP #$26
        BEQ TST3         ;WAIT FOR IRQ FROM TIMER
        SEI
        LDA #$28
        STA PBD           ;STOP COUNTER 1, START COUNTER 2, START TIMER
        LDA PAD
        CPX #$38
        BCC RTN1         ;COLLECT DATA FOR 20 CHANNELS
        LDA SCANH
        CMP #$10
        BEQ JMPTY
JMPTY   JMP SYS1         ;RETURN FOR NEW TRIGGER PULSE AFTER 20 CHANNELS
        JMP TTYOUT       ;OUTPUT DATA AFTER 10000 SCANS
        *=$02F9
        ;
        ;IRQ SERVICE ROUTINE FOR TIME-OUT
LOOP1   LDY #01          ;THIS LOOP IS USED TO INCREASE CHANNEL WIDTHS
        DEY              ;BY STORING VARIOUS VALUES AT LOCATION $02FA
        CPY #01
        BCS LOOP1
        SEC
        SBC #$20
        STA PBD           ;RESET TIMER
        RTI
        ;
        ;DATADD

```

```

;24 BIT DECIMAL DATA STORAGE ROUTINE
;FIRST BYTE IS LCW CRDER BYTE
DATADD CLC
        LSR A           ; SHIFT DATA FROM 4 MSB
        LSR A           ; TO 4 LSB
        LSR A
        LSR A
        CLC
        SED
        ADC DATA,X     ;ADD TO LOW ORDER BYTE
        STA DATA,X
ADD1    INX
        BCC DAT1
        CLC
        LDA DATA,X     ;INCREMENT NEXT BYTE IF CARRY OCCURS
        ADC #01
        STA DATA,X
        INX
        BCC DAT2
        CLC
        LDA DATA,X
        ADC #01
        STA DATA,X
        CLC             ;INCREMENT HIGH ORDER BYTE IF NECESSARY
        JMP DAT2
DAT1    INX             ;INCREMENT MEMORY POINTER FOR NEXT CHANNEL
DAT2    INX
        RTS
        *=$0380
        ;
        ;TTYOUT
;OUTPUT ROUTINE FOR ROSSI-ALPHA DATA
;ROUTINE IS EXECUTED AFTER 100000 SCANS OR IN RESPCNSE TC NMI
TTYOUT JSR INIT1
        JSR CRLF

```

```

LDA #02
STA CT
JMP TT1
LP2 CLD
CLC
ADC #03 ;DATA IS IN DECIMAL FORM IN THREE BYTES
STA CT
TT1 TAX
LDY #00
LP1 STX TMPX
STY TMPY
LDA DATA,X ;GET DATA BYTE
JSR PRTBYT
LDX TMPX
LDY TMPY
DEX ;SET DATA INDEX FOR NEXT LOWER CRDER BYTE
INY
CPY #03
BMI LP1 ;LEAVE LOOP AFTER THREE BYTES ARE OUTPUT
JSR CRLF
LDA CT
CMP #$3E ;LEAVE AFTER ALL DATA HAS BEEN OUTPUT
BCC LP2 ;LAST 3 BYTES CONTAINS NUMBER OF SCANS
JSR CRLF
JMP BKGND
*=$0010
;
;BKGND
;ROUTINE TO COUNT UNCORRELATED NEUTRON EVENTS
BKGND SEI
LDA #00 ;INITIALIZE DATA PORTS
STA PADD
STA BGLL
STA BGL
STA BGH

```

```

STA BKGLL
STA BKGL
STA BKGH
LDA #$3F
EKG2 STA PBDD ;LOWER 6 BITS OF PORT B ARE OUTPUTS
LDA #$04
STA PBD ;RESET COUNTER 2
LDA #$28
STA PBD ;ENABLE COUNTER 2, START TIMER
CLI
TIRQ CMP #$28
BEQ TIRQ ;WAIT FOR IRQ FROM TIMER
SEI
LDA #00
STA PBD ;STOP COUNTER 2
SED
LDA PAD ;GET DATA FROM COUNTER
CLC
LSR A ;SHIFT DATA TO ELIMINATE COUNTS FROM COUNTER 1
LSR A
LSR A
LSR A
CLC
ADC BKGLL ;ADD DATA TO LOW ORDER BYTE
STA BKGLL
BCC BKG3
CLC
LDA BKGL
ADC #012 ;INCREMENT NEXT BYTE IF CARRY OCCURS
STA BKGL
BCC BKG3
CLC
LDA BKGH
ADC #01 ;INCREMENT HIGH ORDER BYTE IF NECESSARY
STA BKGH

```

```

EKG3      CLC
          LDA BGLL          ;INCREMENT SCAN COUNTER
          ADC #01
          STA BGLL
          BCC BKG1
          CLC
          LDA BGL
          ADC #01
          STA BGL
          BCC BKG1
          CLC
          LDA BGH
          ADC #01
          STA BGH
EKG1      CLC
          LDA BGH
          CMP SCANH        ;CONTINUE COUNTING UNTIL NUMBER OF BACKGROUND SCANS
          BCC BKG2        ;AND NUMBER OF DATA SCANS ARE EQUAL
          CLC
          LDA BGL
          CMP SCANL
          BCC BKG2
          CLC
          LDA BGLL
          CMP SCANLL
          BCC BKG2
          JSR INIT1       ;OUTPUT BACKGROUND COUNT AND NUMBER OF SCANS
          JSR CRLF
          JSR CRLF
          LDA BKGH
          JSR PRTBYT
          LDA BKGL
          JSR PRTBYT
          LDA BKGLL
          JSR PRTBYT

```

```
JSR CRLF
LDA BGH
JSR PRTBYT
LDA BGL
JSR PRTBYT
LDA BGLL
JSR PRTBYT
JSR CRLF
HERE JMP HERE
•END
```

XI. APPENDIX D:

DATA COLLECTION ROUTINE VARMEN.SRC

A. Description of VARMEN.SRC

A flowsheet of routine VARMEN.SRC is shown in Figure 11.1 while a listing of this routine may be found in section B of this appendix. Execution always begins with routine ZEROM which zeros the memory corresponding to the channels. Routine SYSINT (a modified version of what was used in ROSSI.SRC) then performs the necessary PIA initializations. Since the variance to mean method does not require a trigger neutron detection a single scan of 1024 channels follows immediately.

The 1024 channels are located within 512 bytes. Since each counter used four bits this is a very convenient and efficient method of obtaining a large number of channels in a small memory. Data collected in counter 1 are shifted to the most significant four bits of the byte and then stored in memory. The data from counter 2, corresponding to the next channel, are shifted to the least significant four bits of the data byte and added to the memory location containing the data from counter 1. The memory pointer (Y index register) is then incremented for the next two channels. The shifting process eliminates counts from the active counter in addition to putting the channels in the proper sequence.

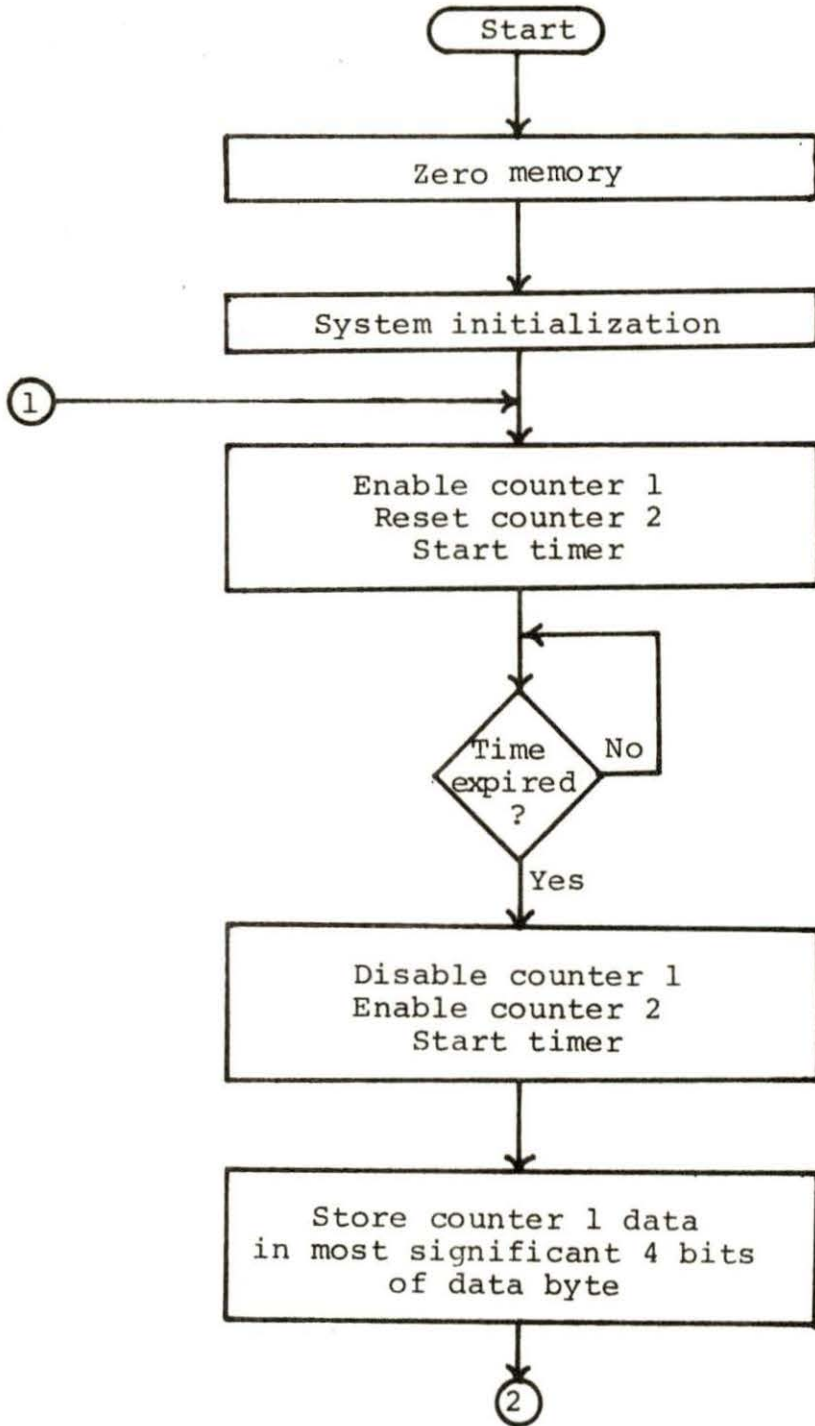


Figure 11.1. Flowsheet for VARMEN.SRC

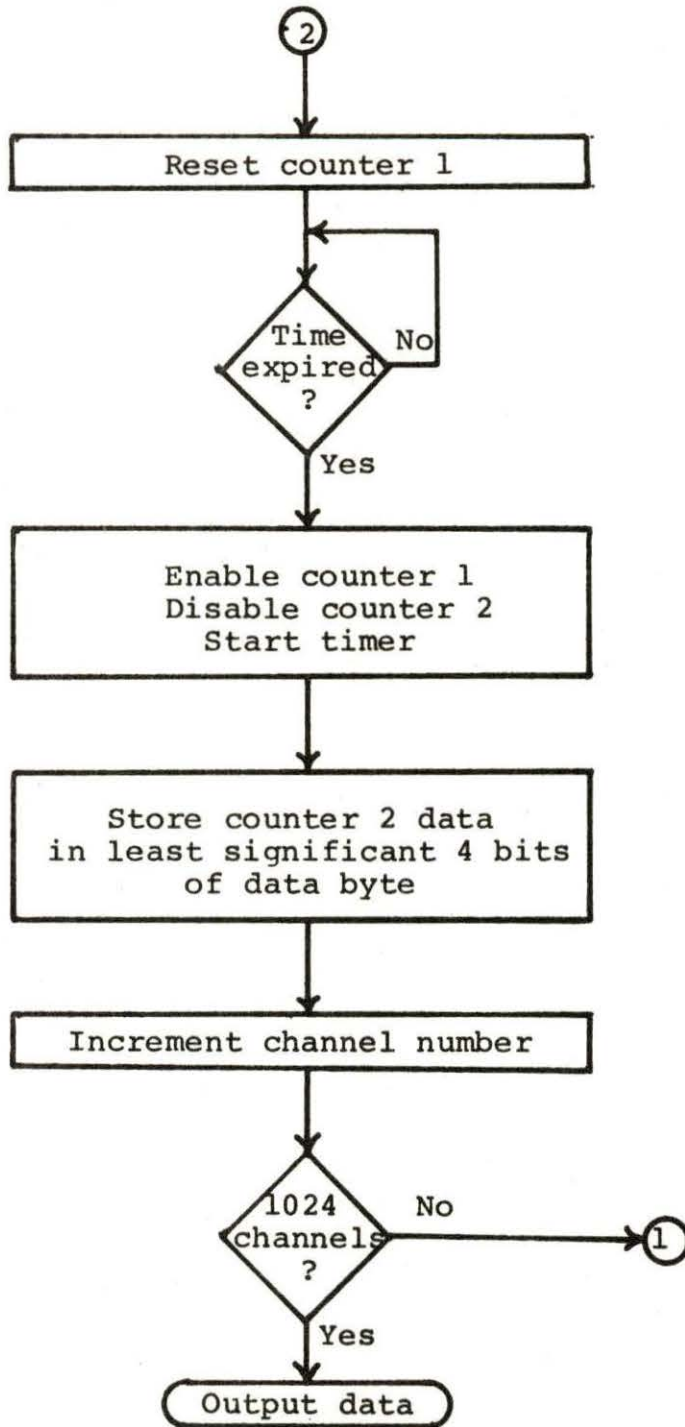


Figure 11.1 continued

The timer algorithm is identical to that used in ROSSI.SRC and therefore the comments dealing with channel width deviation apply to VARMEN.SRC also. The only difference is that channel widths (or gate times) are dependent upon the value stored at location \$00E1.

Upon completion of the 1024 channel scan the data are output to paper tape. A carriage return and line feed occurs every 64 channels. After 1024 channels have been output a control D is appended to the paper tape. The 64 character record is used to provide convenient card images for the paper tape reader in the Iowa State University computation center. The control D character is used to signal the end of the data set. In addition to this special format, the data set is flanked by approximately 32 inches of paper tape leader for handling purposes.

B. Source Code Listing
of VARMEN.SRC

```

;VARMEN.SRC
;THIS ROUTINE COLLECTS DATA TO ALLOW A VARIANCE-TO-MEAN ANALYSIS
;FOR DETERMINATION OF PROMPT NEUTRON DECAY CONSTANTS.
;DATA IS ACQUIRED BY STORING THE NUMBER OF COUNTS OBTAINED IN EACH
;INDIVIDUAL CHANNEL RESULTING FROM A SINGLE SCAN OF 1024 CHANNELS.
;CHANNEL WIDTH IS DETERMINED BY THE VALUE STORED AT LOCATION $00E1.
;THE DEFAULT VALUE IS 176 MICROSECONDS.

```

```

;
;*****
;**
;**          CHANNEL WIDTH DATA
;**
;**          CHANNEL WIDTH          HEXIDECIMAL VALUE
;**          (MICROSECONDS)        STORED AT MEMORY
;**                                LOCATION $00E1
;**          176                    01
;**          425                    20
;**          680                    40
;**          925                    60
;**          1190                   80
;**          1450                   A0
;**          1700                   C0
;**          1950                   E0
;**          2200                   FF
;**
;*****
;

```

```

PRTBYT=$1E3B
INIT1=$1E8C
CRLF=$1E2F
OUTCH=$1EA0
DATAL=$0000
DATAH=$0001
TMPY=$0002
COUNT=$0003

```

```

IRQL=$17FE
IRQH=$17FF
PADD=$1701
PBDD=$1703
PAD=$1700
PBD=$1702
;
*=$0004
;ZEROM
;ZERO MEMORY BETWEEN $0200 AND $03FF
LDA #$02
ZRI STA DATAH
LDY #00
TYA
STA DATAL
ZRLP STA (DATAL),Y
INY
CPY #$FF
BCC ZRLP
STA (DATAL),Y
LDA #03
CMP DATAH
BNE ZRI
;
;SYSTEM INITIALIZATION
SYSINT LDX #$FF
TXS ;INITIALIZE STACK POINTER
JSR INIT1
JSR CRLF
CLI
LDA #$3F
STA PBDD ;SET UP LOWER 6 BITS OF PORT B AS OUTPUTS
LDA #00
STA PBD ;DISABLE COUNTERS AND TIMER
STA PADD ;SET UP PORT A AS INPUTS

```

```

STA IRQH
TAY          ;ZERO MEMORY INDEX
LDA #02
STA DATAH  ;SET DATA BASE AT $0200
LDA #$E0
STA IRQL    ;SET IRQ VECTOR AT $00E0
;
;SCAN 1024 CHANNELS (STORE IN 512 BYTES)
SCAN1 LDA #$26
STA PBD     ;ENABLE COUNTER 1, RESET COUNTER 2, START TIMER
TST1  CMP #$26
BEQ TST1    ;WAIT FOR IRQ FROM TIMER
LDA #$28
STA PBD     ;STOP COUNTER 1, ENABLE COUNTER 2, START TIMER
LDA PAD
ASL A      ;SHIFT DATA TO ELIMINATE COUNTS FROM COUNTER 2
ASL A
ASL A
ASL A
STA (DATA),Y ;STORE DATA FROM COUNTER 1 IN MOST SIGNIFICANT 4 BITS
LDA #$29
STA PBD     ;RESET COUNTER 1
TST2  CMP #$29
BEQ TST2    ;WAIT FOR IRQ FROM TIMER
LDA #$22
STA PBD     ;STOP COUNTER 2, ENABLE COUNTER 1, START TIMER
LDA PAD
LSR A      ;SHIFT DATA TO ELIMINATE COUNTS FROM COUNTER 1
LSR A
LSR A
LSR A
CLC
ADC (DATA),Y ;STORE DATA FROM COUNTER 2 IN LEAST SIGNIFICANT 4 BITS
STA (DATA),Y
CPY #$FF

```

```

      BCC PGM1
      LDA #03
      CMP DATAH
      BEQ OUTPUT
      STA DATAH
      LDY #00
      JMP SCAN1
PGM1  INY
      JMP SCAN1
      ;
      ;TTY OUTPUT ROUTINE
      ;THIS ROUTINE OUTPUTS DATA AFTER SCANNING 1024 CHANNELS
      ;DATA IS OUTPUT TO PAPER TAPE IN A FORMAT THAT
      ;THE ITEL AS/5 MIGHT UNDERSTAND
OUTPUT JSR INIT1
      JSR LEADER
      LDA #02
      STA DATAH
      LDA #$20
      STA COUNT
TT2   LDY #00
TTLP  TYA
      STA TMPY
      LDA (DATA),Y
      JSR PRTBYT
      DEC COUNT
      LDA #00
      CMP CCOUNT
      BNE TT3
      LDA #$20
      STA COUNT      ;OUTPUT CR/LF AFTER 32 BYTES (64 PCINTS)
      JSR CRLF
TT3   LDY TMPY
      CPY #$FF
      BCS TT1

```

```

      INY
      JMP TTLP
TT1   LDA #03
      CMP DATAH
      BEQ DONE
      STA DATAH
      JMP TT2
DONE  LDA #$04           ;APPEND CNTRL/D (EOT) TO DATA
      JSR DUTCH
      JSR LEADER
HERE  JMP HERE
      ;
      ;SUBROUTINE LEADER
      ;ADDS APPROXIMATELY 32 INCHES OF LEADER TO PAPER TAPE
LEADER LDX #00
LEADLP LDA #00
      JSR DUTCH
      LDA #00
      JSR DUTCH
      INX
      CPX #$A0
      BCC LEADLP
      RTS
      *=$00E0
      ;
      ;IRQ SERVICE ROUTINE FOR TIMER
LOOP  LDX #01           ;THIS LOOP IS USED TO VARY THE CHANNEL WIDTH
      DEX             ;BY STORING VARIOUS VALUES AT MEMORY LOCATION $00E1
      CPX #01
      BCS LOOP
      SEC
      SBC #$20
      STA PBD         ;RESET TIMER
      RTI
      .END

```